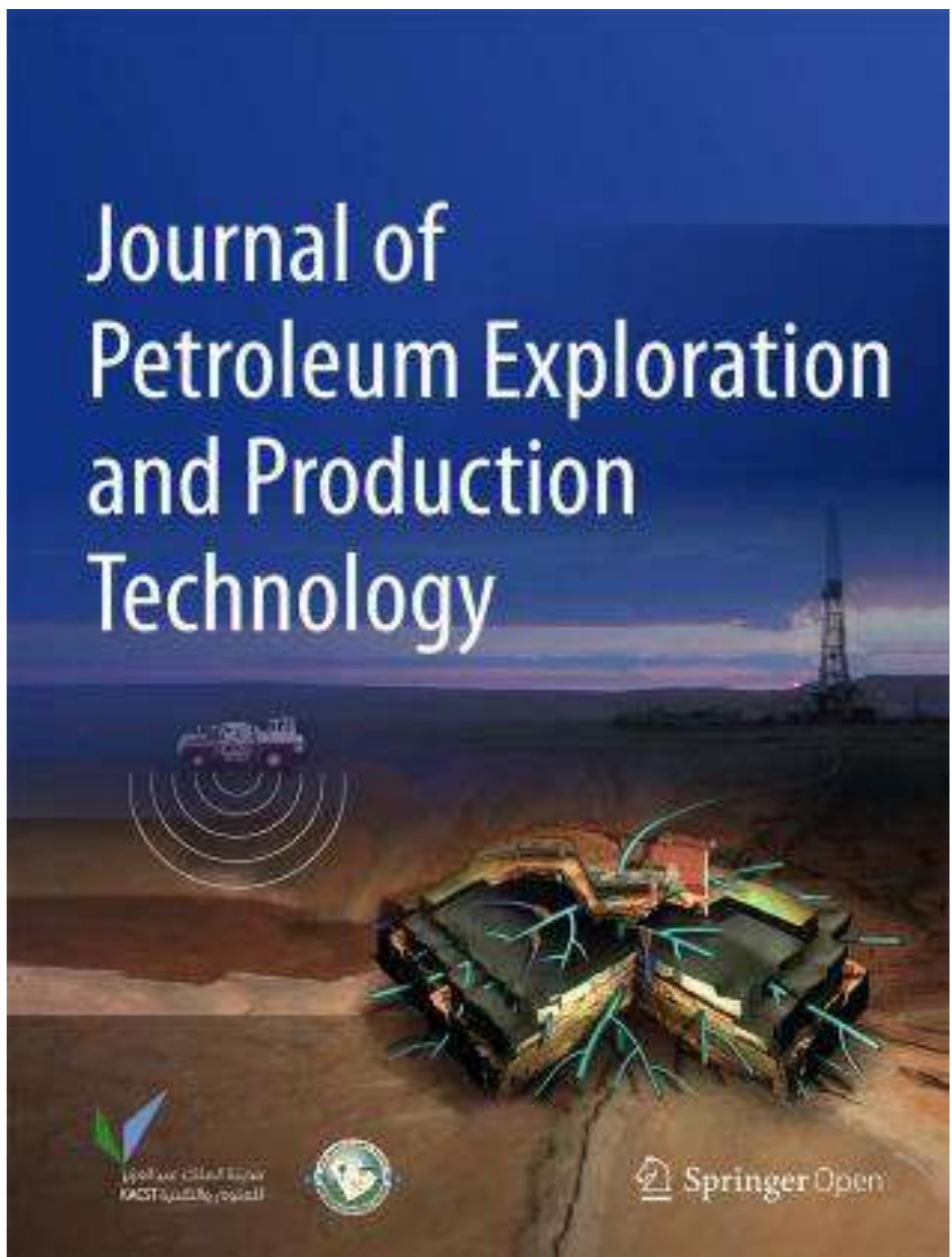



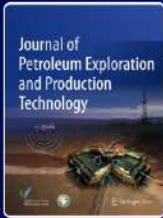
# Journal of Petroleum Exploration and Production Technology



المجلة الدولية للتكنولوجيا  
FACTA INTERNATIONAL JOURNAL  
OF PETROLEUM TECHNOLOGY



 Springer Open



# Journal of Petroleum Exploration and Production Technology

Publishing model  
[Open access](#)

Submit your manuscript →

[Explore open access funding](#) | [Select institution](#)

About this journal ▾ Articles ▾ For authors ▾ Journal updates

## Overview

The Journal of Petroleum Exploration and Production Technology is an international open access journal that publishes leading edge studies in the field of petroleum engineering, petroleum geology and exploration geophysics and the implementation of related technologies to the development and management of oil and gas reservoirs from their discovery through their entire production cycle.

### Journal metrics

- Journal Impact Factor 3.2 (2024)
- 5-year Journal Impact Factor 2.8 (2024)

# Editorial Board

<https://link.springer.com/journal/13202/editorial-board>

[Home](#) > [Journal of Petroleum Exploration and Production Technology](#) > [Editorial board](#)



## Journal of Petroleum Exploration and Production Technology

Publishing model

[Open access](#)

[Submit your manuscript](#) →

[Explore open access funding](#) | [Select institution](#)

[About this journal](#) ▾ [Articles](#) ▾ [For authors](#) ▾ [Journal updates](#)

### Editorial board

#### Emeritus Editor-in-Chief



**Professor Ali Ghalambor PhD**

American Petroleum Institute, Washington, United States, retired 2010

#### Assistant Editor-in-Chief



**Rahman Ashena PhD**

SEDA-Group, North America, United States

#### Associate Editors



**Abd el-aziz Khairy Abd el-eal PhD**

Kuwait Institute for Scientific Research, Kuwait City, Kuwait



**Ahmad Abushaikha PhD**

Hamad bin Khalifa University, Doha, Qatar



**Abdullah Almansour PhD**

National Center for Petroleum Technology and Mining, Riyadh, Saudi Arabia



**Zuhair A. AlYousef PhD**

Saudi Aramco (Saudi Arabia), Dhahran, Saudi Arabia



**Vasile Badiu PhD**

SPE Local and Global Committees, Ploiești, Romania



**Santanu Banerjee PhD**

Indian Institute of Technology Bombay, Mumbai, India



**Hadi Belhaj PhD**

Khalifa University of Science and Technology, Abu Dhabi, United Arab Emirates



**Mohamed A.K. El-Ghali PhD**

Sultan Qaboos University, Muscat, Oman



**Ming Feng PhD**

Pennsylvania State University, State College, United States

# Editorial Board

<https://link.springer.com/journal/13202/editorial-board>



**Amin Gholami PhD**

National Iranian Oil Company (Iran), Tehran, Iran



**Foad Haeri PhD**

National Energy Technology Laboratory, South Park Township, United States



**Erfan Hosseini PhD**

National Iranian Oil Company (Iran), Tehran, Iran



**Ibtelwaleed Hussein PhD**

Qatar University, Doha, Qatar



**Wei Lin PhD**

School of Geosciences, Yangtze University, Jingzhou, China



**Tianshou Ma PhD**

Southwest Petroleum University, Chengdu, China



**Debotyam Maity PhD**

Gas Technology Institute, Des Plaines, United States



**Zohreh Movahed PhD**

Schlumberger, Kuala Lumpur, Malaysia



**Saeed Mozaffari PhD**

Virginia Tech, Blacksburg, United States



**Changhyup Park PhD**

Kangwon National University, Chuncheon, South Korea



**Ahmed E. Radwan PhD**

Jagiellonian University, Krakow, Poland



**Ahmad Sakhaee-Pour PhD**

University of Houston, Houston, United States



**Weijun Shen PhD**

Chinese Academy of Sciences, Beijing, China



**Amin Shokrollahi PhD**

University of Adelaide, Adelaide, Australia



**Zheng Sun PhD**

China University of Mining and Technology, Xuzhou, China



**Fengrui Sun PhD**

China University of Petroleum, Beijing, Beijing, China



**Qian Sun PhD**

New Mexico Institute of Mining and Technology, Socorro, United States



**Hung Vo Thanh PhD**

Seoul National University, Seoul, South Korea

## Editorial Board

<https://link.springer.com/journal/13202/editorial-board>



**Sen Wang PhD**

China University of Petroleum, East China, Qingdao, China



**Zhihua Wang PhD**

Northeast Petroleum University, Daqing, China



**Tao Zhang PhD**

Southwest Petroleum University, Chengdu, China



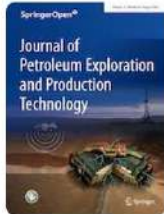
**Fengyuan Zhang PhD**

China University of Petroleum, Beijing, Beijing, China



**Xin Zhao PhD**

China University of Petroleum, East China, Qingdao, China



Volume 15, Issue 8  
August 2025

9 articles in this issue

**Spectral decomposition-based static reservoir simulations image Cretaceous hydrocarbon-bearing incised-valley, Southwest Pakistan**

Muhammad Tayyab Naseer, Sultan Alshehery ... Assimina Antonarakou  
Original Paper - Exploration Geophysics | Open access | 02 August 2025 | Article: 132



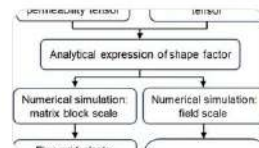
**Accurate estimation of permeability reduction resulted from low salinity water flooding in clay-rich sandstones**

Xiaojuan Zhang, Muntadher Abed Hussein ... Ahmad Khalid  
Original Paper - Production Engineering | Open access | 02 August 2025 | Article: 131



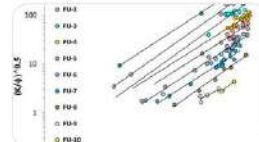
**A new shape factor for counter-current imbibition in anisotropic matrix blocks of fractured reservoirs**

Guanlin Li, Yuhu Bai & Yuetian Liu  
Original Paper - Production Engineering | Open access | 28 July 2025 | Article: 130



**Assessing pore quality impact on saturation exponent and water saturation calculation**

Suryo Prakoso, Muhammad Burhannudinnur ... Billy Arioseno Prakoso  
Original Paper - Production Engineering | Open access | 24 July 2025 | Article: 129





**Application of neural architecture search in lithology identification**

Yuhao Zhang, Hanmin Xiao ... Jianbo Tan

**Original Paper – Exploration Geology** | Open access | 23 July 2025 | Article: 128

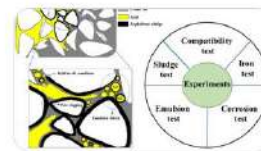
Sample	Actual Lithology	Identified Lithology	Confidence
1	Sandstone	Sandstone	0.95
2	Sandstone	Sandstone	0.92
3	Sandstone	Sandstone	0.98
4	Sandstone	Sandstone	0.91
5	Sandstone	Sandstone	0.93
6	Sandstone	Sandstone	0.94
7	Sandstone	Sandstone	0.96
8	Sandstone	Sandstone	0.97
9	Sandstone	Sandstone	0.99
10	Sandstone	Sandstone	0.90

**Optimizing demulsifier selection for crude oil dehydration: a fuzzy TOPSIS-based multi-criteria decision-making approach**

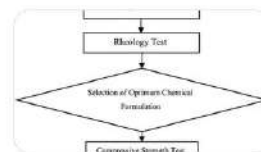
Jianyong Yu, Merwa Alhadrawi ... M. Mehdi Shafieezadeh

**Original Paper – Production Engineering** | Open access | 23 July 2025 | Article: 127**Formation damage analysis of matrix acidizing: effect of emulsion formation, asphaltene sludge, and iron precipitation**

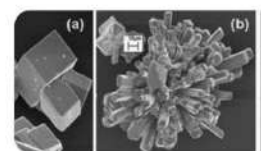
Shayan Zarei, Afshin Bahri ... Arezou Jafari

**Original Paper – Production Engineering** | Open access | 19 July 2025 | Article: 126**A polymer-crosslinker-nanoparticles formulation for effective sand consolidation in loose sandstone formations**

Mysara Eissa Mohyaldinn, Emmanuel Bullen Lado Solomon ... Mohammed A. Ayoub

**Original Paper – Production Engineering** | Open access | 14 July 2025 | Article: 125**Synchronous impact of divalent ions on formation damage and wettability alteration during smart water injection: static and dynamic assessment**

Mohammad Reza Esmailinasab, Mastaneh Hajipour ... Mohammad Behnood

**Original Paper – Production Engineering** | Open access | 12 July 2025 | Article: 124



# Assessing pore quality impact on saturation exponent and water saturation calculation

Suryo Prakoso<sup>1</sup> · Muhammad Burhannuddinur<sup>2</sup> · Firman Herdiansyah<sup>2</sup> · Sigit Rahmawan<sup>1</sup> · Billy Arioseno Prakoso<sup>1</sup>

Received: 22 September 2024 / Accepted: 9 June 2025  
 © The Author(s) 2025

## Abstract

The saturation exponent is one of the most important parameters needed to calculate water saturation in Archie's equation. Generally, the saturation exponent is considered constant, but not all depth intervals have the same characteristics. This study aims to investigate the relationship between rock quality and the saturation exponent, a critical parameter in Archie's equation for water saturation calculation. Given that rock texture and pore characteristics vary significantly with depth, assuming a constant saturation exponent can lead to inaccurate results. The study integrates core analysis and petrographic data to classify rock quality and its relationship with the saturation exponent.  $R_t$  and  $R_o$  data from core analysis are used to determine saturation exponent. Furthermore, rock quality is identified using the hydraulic flow unit concept by constructing log-log plots of reservoir quality index and pore volume to grain volume ratio. Several pore attribute parameters, such as the combination of shape factor and tortuosity (Kozeny's constant), specific surface area, reservoir quality index, and clay volume, are examined for their influence on the saturation exponent. The saturation exponent shows strong correlation with Kozeny's constant and clay volume. An empirical equation was developed to estimate the saturation exponent based on these parameters. Using this empirical equation, the saturation exponent can be estimated across depth intervals, leading to more accurate water saturation calculations. This study offers a practical method to estimate saturation exponent variation using readily available log-derived parameters. It contributes to more reliable determination of saturation exponent variation and enhances the accuracy of water saturation calculations in heterogeneous formations.

**Keywords** Konzeny constant · Saturation exponent · Shape factor · Tortuosity · Reservoir quality index

## Nomenclatures

### Latin letters

$a$	Tortuosity factor
$c$	Kozeny constant
$m$	Cementation exponent
$n$	Saturation exponent
$A$	Empirical constants
$B$	Empirical constants
$C$	Empirical constants
$F$	Formation factor

$F_s$	Shape factor
$K$	Permeability, mD
$R_o$	Rock resistivity filled 100% water, Ohm-m
$R_t$	Measured rock resistivity, Ohm-m
$R_w$	Water resistivity, Ohm-m
$S_w$	Water saturation, fraction
$S_{vgr}$	Specific internal surface area per unit grain volume, cm <sup>2</sup> -l or μm <sup>2</sup> -l
$S_b$	Specific internal surface area per unit bulk volume, cm <sup>2</sup> -l or μm <sup>2</sup> -l
$T$	Tortuosity
$V_{clay}$	Volume clay, fraction

✉ Suryo Prakoso  
[suryo\\_prakoso@trisakti.ac.id](mailto:suryo_prakoso@trisakti.ac.id)

<sup>1</sup> Petroleum Engineering, Faculty of Earth and Energy Technology, Universitas Trisakti, Jakarta, Indonesia

<sup>2</sup> Geological Engineering, Faculty of Earth and Energy Technology, Universitas Trisakti, Jakarta, Indonesia

## Greek letter

$\phi$	Porosity, fraction
$\phi_z$	Ratio of pore volume to grain volume

## Acronyms

CEC	Cation exchange capacity, meq/g
-----	---------------------------------



<i>FU</i>	Flow unit
<i>FZI</i>	Flow zone indicator
<i>RI</i>	Resistivity index
<i>RQI</i>	Reservoir quality index
<i>SCAL</i>	Special core analysis
<i>XRD</i>	X-ray diffraction

## Introduction

The saturation exponent ( $n$ ) is one of the most fundamental parameters for calculating water saturation using Archie's equation (Shi-jun 2009). If obtaining the saturation exponent ( $n$ ) from core measurements is not possible, it is typically assumed to be a constant value, usually 2. In most cases, the water saturation calculation for the entire depth interval is represented by a constant saturation exponent (Al-Otaibi et al. 2012). However, under certain conditions, assuming this constant value can lead to significant errors in the calculated water saturation.

In sandstone, the sedimentation process and depositional environment significantly influence the variability of the reservoir's physical properties and rock quality (Abu-Hashish et al. 2022; Abu-Hashish and Afify 2022; Abu-Hashish and Ali 2021). This variability indicates that the saturation exponent cannot be represented by a single constant value (Hamada et al. 2002; Yadav et al. 2017). In shaly sandstone, the clay volume fraction, as well as clay minerals with varying conductivity, show a significant effect on the saturation exponent (Fan et al. 2020; Kurniawan and Bassiouni 2007). The uncertainty in the saturation exponent ( $n$ ) may be caused by the complexity of pore geometry and pore type, structural heterogeneity, along with variations in wettability (Kumar et al. 2010).

Several factors can contribute to the saturation exponent uncertainty. Some studies suggest that the type of porosity not only affects the cementation factor ( $m$ ) but also the saturation exponent (Olusola and Aguilera 2013; Tian et al. 2022, 2024; Watfa 1991). Variations in the rock's microstructure, such as reservoir heterogeneity, wettability, and rock texture (Acosta et al. 2021; Adisoemarta et al. 2001), can influence the resistivity index and cause uncertainty in determining the saturation exponent. The presence of rock microstructure leads to pore complexity, characterized by pore geometry and structure, which affect pore space connectivity and wettability. Lower pore area and tortuosity contribute to a decrease in the saturation exponent (Zhang et al. 2021). Variations in the saturation exponent related to pore geometry effects can result in errors exceeding 10 saturation units in water saturation evaluation (Stalheim and Eidesmo 1995; Watfa 1991; Worthington and Pallatt 1990).

Changes in wettability conditions can affect fluid distribution within the pores space of rock, influencing resistivity response and complicating the estimation of the saturation exponent (AL-Dujaili et al. 2023; Donaldson and Siddiqui 1989). The rock's wettability preference has significant impacts on water saturation and saturation exponent (Sondena et al. 1992). The presence of authigenic clay increases oil-wet characteristics and affects the saturation exponent (Corbett and Mousa 2010; Rabiee and Hamada 2022; Shi-jun 2009).

Various methods have been used by researchers to determine the saturation exponent ( $n$ ), such as regression approaches involving water saturation and porosity (Hamada et al. 2002), and resistivity (Al-Hilali et al. 2015; Corbett and Mousa 2010). The saturation exponent describes how the rock's resistivity changes with varying water saturation (Adisoemarta et al. 2001; Olusola and Aguilera 2013; Venkataramanan et al. 2016). Differences in water saturation for heterogeneous reservoirs indicate changes in wettability, which are directly related to the saturation exponent (Adisoemarta et al. 2001). The change in wettability is linearly correlated with the change in the saturation exponent (Donaldson and Siddiqui 1989).

This study aims to determine the value of the saturation exponent by considering heterogeneity and differences in rock quality. The variation in the saturation exponent with respect to heterogeneity and differences in rock quality are not yet fully understood, creating the need for a more comprehensive approach that takes into account the parameters influencing rock quality. The integration of petrographic analysis, routine core analysis, and special core analysis data is used to develop a model that more comprehensively considers for this variability. The variable saturation exponent values obtained from this approach are expected to provide more accurate water saturation estimates in a simpler manner.

## Data and methods

### Data

This study uses sandstone data from the Central Sumatra Basin. The general lithological description consists of sandstone with grain sizes ranging from coarse to fine, with good to poor sorting, expected to represent the overall rock group. The research utilizes both routine core and *SCAL* data, including porosity, permeability, and resistivity index. The routine core data consists of porosity and permeability, while special core analysis (*SCAL*) data includes the formation factor and resistivity index. Sedimentological data, such as petrography (thin sections) and X-ray diffraction (*XRD*),

are also incorporated. The routine core data show variations in porosity and permeability (Table 1). The porosity data ranges from 4.5 to 36.9%, permeability data ranges from 0.12 to 33,400 mD, and clay volume is below 20%.

## Methods

### Formation resistivity factor and resistivity index

Archie formulated an equation to describe the resistivity behavior of reservoir rock based on core data measurements conducted in the laboratory (Archie 1942). Equation 1 determines the resistivity of rock that is fully saturated with formation water. The Formation Factor ( $F$ ) is defined as the ratio of the resistivity of rock that is 100% saturated with saline water to the resistivity of saline water  $R_w$ .

$$F = \frac{R_o}{R_w} = \frac{a}{\phi^m} \quad (1)$$

Archie's Eq. 2 describes the change in resistivity caused by hydrocarbon saturation. Archie defines the resistivity index,  $RI$ , as the ratio of the measured resistivity of the rock,  $R_t$ , to the resistivity of the rock when it is 100% saturated with formation water  $R_o$ .

$$RI = \frac{R_t}{R_o} = \frac{1}{S_w^n} \quad (2)$$

Where  $F$  is the Formation Factor,  $R_o$  is the resistivity of the rock 100% saturated with water,  $R_w$  is the water resistivity,  $\phi$  is the porosity,  $R_t$  is the true resistivity of the rock,  $S_w$  is the water saturation,  $a$  is the tortuosity factor,  $m$  is the cementation exponent, and  $n$  is the saturation exponent.

The ratio  $R_t/R_o$  is known as the resistivity index ( $RI$ ), which is primarily influenced by the salinity of the formation water (Tiab and Donaldson 2015). Although  $RI$  is generally considered to be unity at 100%  $S_w$ , many researchers have experimentally agreed that this value is not unity (Ara et al. 2001; Chen et al. 2002; Tiab and Donaldson 2015).

Equation 1 can be rearranged as follows:

$$\text{Log } F = \text{Log } a - m \text{Log } \phi \quad (3)$$

When the formation factor data is plotted against porosity on a log-log graph, drawing a line through the point (1,1)

and not through the point (1,1) produces a slope that represents the cementation exponent ( $m$ ).

Equation 2 can be rearranged as follows:

$$-n \text{Log } S_w = \text{Log } 1/I \quad (4)$$

On a log-log graph, plotting the resistivity index against saturation, drawing a line from the point (1,1) will produce a slope that represents the saturation exponent ( $n$ ).

### Rock quality grouping

Reservoir quality grouping is the process of characterizing reservoir rocks based on their dynamic behavior. The dynamic behavior of a group of rocks are determined by studying the complexity of the pore space through texture, rock fabric, diagenetic processes, and the interaction between the rock itself and the fluid (Al-Dujaili 2023). El-Khatib demonstrated that rock samples with similar capillary pressure curves should have the same tortuosity ( $\tau$ ) and irreducible water saturation ( $S_{wi}$ ) (El-Khatib 1995). Similarities in pore architecture are reflected by similarities in pore shape and tortuosity, where the combination of these two pore attributes are known as the Kozeny constant (Kozeny 1927). Amaefule rearranged the Kozeny equation as follows (Amaefule et al. 1993):

$$\left(\frac{K}{\phi}\right)^{0.5} = \frac{1}{S_{vgr} \sqrt{F_s \tau}} \left(\frac{\phi}{1-\phi}\right) \quad (5)$$

Where  $K$  is permeability,  $\phi$  is porosity,  $F_s$  is the shape factor,  $\tau$  is tortuosity, and  $S_{vgr}$  is the specific internal surface area.  $(k/\phi)^{0.5}$  describes the pore geometry, representing the mean hydraulic radius, which is known as the Reservoir Quality Index ( $RQI$ ), and  $\frac{1}{S_{vgr} \sqrt{F_s \tau}}$  represents the Flow Zone Indicator ( $FZI$ ). Equation 5 can be rearranged as follows:

$$RQI = FZI (\phi_z) \quad (6)$$

$\phi_z$  is the ratio of pore volume to grain volume as follows:

$$\phi_z = \left(\frac{\phi}{1-\phi}\right) \quad (7)$$

Equation 6 can be written in log-log form as follows:

$$\text{Log } RQI = \text{Log } FZI + \text{Log } (\phi_z) \quad (8)$$

Equation 8 produces a straight line on a log-log plot of  $RQI$  vs.  $\phi_z$ . The intercept of the straight line at  $\phi_z = 1$  represents the Flow Zone Indicator ( $FZI$ ). Samples with different  $FZI$  values will lie on parallel lines.  $FZI$  indicates similarity in

**Table 1** Data used in the study

Number of samples				Rock properties	
Routine Core	SCAL	Petrography	XRD	Porosity %	Permeability mD
104	104	45	45	4.5–36.9	0.12–33,400

pore throat characteristics, which corresponds to the flow unit. Rocks composed of fine grains and poor sorting tend to have a large surface area and high tortuosity, resulting in a low *FZI* value. Conversely, coarse-grained, non-shaly, and well-sorted rocks tend to have smaller surface areas and lower tortuosity, resulting in a higher *FZI* values (Al-Dujaili et al. 2021).

### Study's workflow

Table 2 outlines the research steps undertaken to achieve the objectives of this study. The first step involves obtaining the necessary data for the research. This data is acquired through laboratory measurements following standard rock analysis procedures, including selecting rock samples,

**Table 2** Research Steps

Step 1		Obtaining research data	
Rock Sample Selection	⇒	Number of Samples	⇒ Laboratory Analysis
Determine and select the representative sandstone samples that represent variations in depositional environment, stratigraphy, and mineralogy.		a. Determine the number of samples to be tested based on the research objectives and the required data. b. Ensure that the selected samples represent variations that describe heterogeneity.	Analyze the required parameters, namely lithology, texture and mineralogy through petrographic analysis. Measure the physical properties of rocks, namely porosity and permeability, Resistivity index and capillary pressure through routine core analysis and special core analysis.
Target Output		Obtaining representative research data to evaluate the saturation exponent parameters.	

Step 2		Conduct analysis and integrate data to obtain sufficient information to establish a relationship between rock quality and saturation exponent.	
Lithology and Texture Analysis	⇒	Rock Quality Identification	⇒ Determination of Saturation Exponent Parameters
Determine lithology, dominant texture and mineralogy and identify rock heterogeneity and quality.		Using porosity and permeability data to identify rock quality using the hydraulic flow unit concept.	Processing resistivity index data to obtain saturation exponent and analyzing the influence of petrophysical properties of rock on saturation exponent.
Target Output		Obtaining the most dominant factors influencing heterogeneity, reservoir quality and saturation exponent	

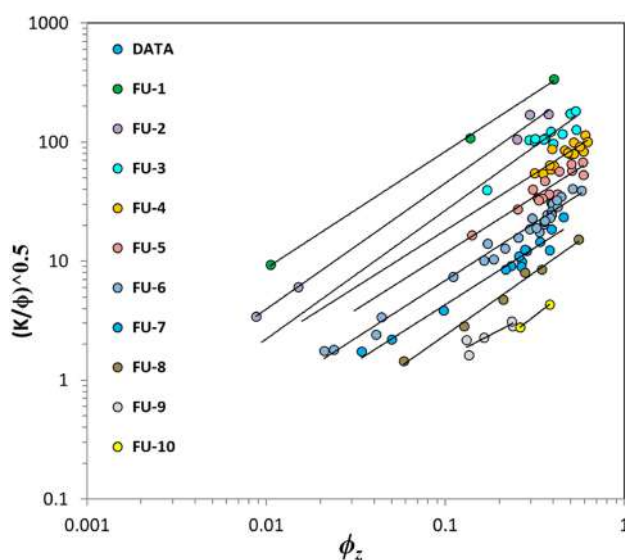
Step 3		Construct a model for estimating the saturation exponent from research findings.	
Data Integration and Analysis	⇒	Factors Affecting Rock Quality	⇒ The Effect of Rock Quality on Saturation Exponent
			⇒ Saturation Exponent Estimation Approach
Obtain an understanding of the effect of heterogeneity on rock quality, as well as its implications for the saturation exponent.		Determining the most dominant factors that influence rock quality including porosity, permeability, clay volume, lithology, texture, pore geometry and internal pore characteristics such as pore shape factor and tortuosity.	Obtaining the relationship and influence of rock quality on the saturation exponent.
Target Output		Obtaining a saturation exponent estimation approach.	

determining the number of samples, and defining the analysis protocols. The second step focuses on data analysis to establish the relationship between rock quality and the saturation exponent. This stage encompasses lithology and texture analysis, rock quality identification, and determining the saturation exponent. The final step involves developing an empirical equation to estimate the saturation exponent based on the research findings. These steps are designed to yield representative results for saturation exponent estimation and ensure accurate water saturation calculations.

## Results and discussion

### Rock quality identification

Rock quality is identified by the similarity of specific surface area, shape factor and tortuosity, known as the Flow Zone Indicator (*FZI*) (Amaefule et al. 1993). A plot between the reservoir quality index ( $((k/\phi)^{0.5})$ ) and the ratio of pore volume to grain volume can separate into several rock groups (Fig. 1). Rock samples can be classified into 10 rock groups based on their pore quality. FU 1 represents a group of rocks with the highest pore quality, while FU 10 represents group of rocks with low quality and high pore complexity. Each rock group shares similar specific surface area, pore shape ( $F_s$ ) and tortuosity. Figure 1 shows that although pore shape ( $F_s$ ) and tortuosity are similar, as the pore space increases, the value of  $(k/\phi)^{0.5}$  also increases.  $(k/\phi)^{0.5}$ , which is known as pore geometry (Wibowo and Permadi 2015), corresponds to the hydraulic pore radius (Kozeny 1927), so the difference within one rock group lies in varying pore sizes. This pore geometry is a characteristic of the pore space directly



**Fig. 1** Identification of rock quality based on the similarity of Flow Zone Indicators

related to rock quality and influences fluid flow (Amaefule et al. 1993; Wibowo and Permadi 2015).

Petrographic data is used to describe the microscopic geological features of each rock group. Table 3 provides an overview of the dominant factors influencing each rock group. Texture is the main factor that differentiates each rock group.

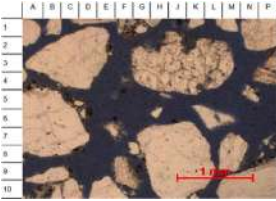

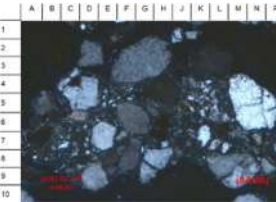
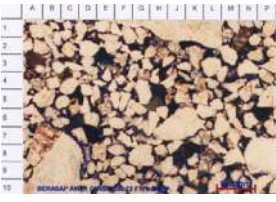
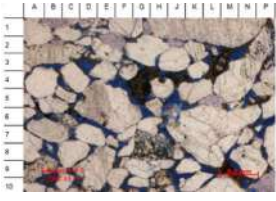
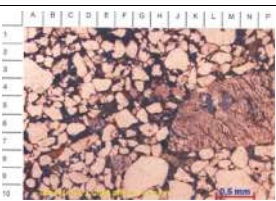
Figure 2 represents the results of petrographic analysis for the best quality of rock group. The petrographic analysis shows that the pore geometry exhibits a loose structure with coarse grains. The observed diagenesis includes pore-filling calcite, kaolinite, pore-lining illite, quartz overgrowth, and a small amount of pyrite. The dissolution of feldspar and matrix has developed into secondary porosity. Based on the SEM data, intensive quartz growth protects the rock from excessive compaction (low-degree compaction), thus preserving primary porosity. Authigenic pyrite partially covers the primary porosity, and kaolinite cement is present in pore spaces and pore channels, but this is minimal. With the development of matrix into secondary porosity and the preservation of primary porosity, this rock has relatively good porosity of 28.8% and permeability in the Darcy range.

Figure 3 represents the results of petrographic analysis for the poorest quality rock group. The petrographic analysis shows that the diagenetic process consists of cementation by quartz overgrowth, illite, kaolinite, and pyrite, followed by the alteration of most unstable grains and matrix into illite, kaolinite, and pyrite. The dissolution of unstable grains has formed secondary porosity. The compaction process, with moderate to high compaction levels, is evident from grain-to-grain contact, indicated by the presence of linear and concavo-convex contacts, as well as pseudo-matrix. The observed porosity in this rock group ranges from poor to moderate, consisting of intergranular porosity, secondary porosity from dissolution, and microporosity that develops between clay minerals. Generally, pore connectivity is poor due to the high content of clay matrix, cementation, and compaction. Pore sizes vary relatively from 2.5 to 60 microns, while microporosity has pore sizes ranging from 0.2 to 1 micron. Kaolinite fills the space between grains as cement. Compaction and cementation are the main factors controlling the decrease in the quality of rock group.

### Formation resistivity factor and resistivity index

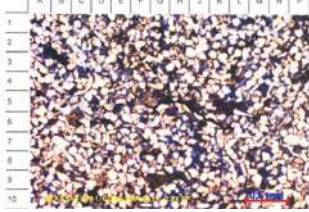
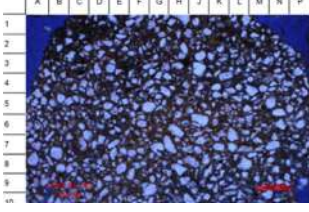
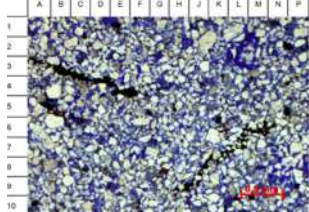

The rock typing method is widely used to classify reservoir rocks into distinct groups based on their specific characteristics. Rocks within each group are deposited under similar geological conditions and undergo similar diagenetic processes. These groups share similarities in pore architecture, which can be identified through microscopic geological features (Wibowo and Permadi 2015). Therefore, each

**Table 3** Microscopic geological feature for each rock group

FU	Microscopic Description	Petrography
FU1	Coarse-grained Sd, mod. sorting, sub-angular to sub-rounded. The dominant mineral is quartz (88%), followed by feldspar (5%), metamorphic rock fragments (4.5%), a small amount of calcite cement and clay minerals	
FU2	Fine-medium-grained sandstone, sub-angular-rounded, poorly sorted. point contact with elongated types. Fragments consist of monocrystalline quartz, a small amount of polycrystalline quartz, microcline, and K-feldspar. Frag. clay (1%) and chert (0.5%). Accessory minerals mica, carbon matrix, and heavy minerals. A small amount of detrital clay matrix and pseudomatrix. Diag. Mod. compaction, point & long contacts. Intergranular & dissolution	
FU3	Loose Sd & Sd, Fine to med., poor to mod.srt, sub-ang. to sub-rnd, point contact, floating & planar. Main component is monocrystalline quartz, fragments polycrystalline quartz, metamorphic fragments, feldspar, and plagioclase. Opaque minerals, small amounts of mica, skeletal planktonic foraminifera, miliolids, small benthics, and detrital clay are also present. Diagenesis compaction, minor precipitation of pyrite within foraminifera chambers, and the replacement calcite, clay minerals & pyrite. Predominantly intergranular	
FU4	Fine to medium-textured Sd, sub-angular to sub-rounded, and moderate Srt. Long & concave-convex contacts. Primary grains are monocrystalline quartz, add. metamorphic and sedimentary frag. Microcline, orthoclase, mica & heavy minerals. Minor pseudomatrix & high-degree compaction. Silica overgrowth, along with kaolinite and siderite replacement. Dissolution secondary porosity.	
FU5	Med.-very coarse Sd, poorly sorted, sub-ang. to sub-rnd. Long & concave-convex Contact. Dominant monocrystalline quartz, add. feldspar (plagioclase and microcline). Minor benthic foraminifera & pseudo-matrix. Detrital clay & carbonate mud. Compaction is strong, with feldspar grain dissolution, minor pyrite precipitation, and clay minerals. Replacement siderite, pyrite, illite, dolomite, calcite, & kaolinite is observed. Intergranular, micro-pores, & dissolution porosity	
FU6	Med-very coarse grain Sd, sub-ang. to sub-rnd., poorly sorted, elongated grain contacts & point contacts. Main components monocrystalline quartz, K-feldspar, shale, silty shale, chert & plagioclase. Skeletal grains from benthic & planktonic foraminifera. Accessory minerals include mica and heavy minerals. Pseudo-matrix is also present, with dispersed distribution and thin laminations. Diagenetic compaction, siderite precipitation, slight replacement of the matrix by siderite, & dissolution. Intergranular & dissolution porosity.	



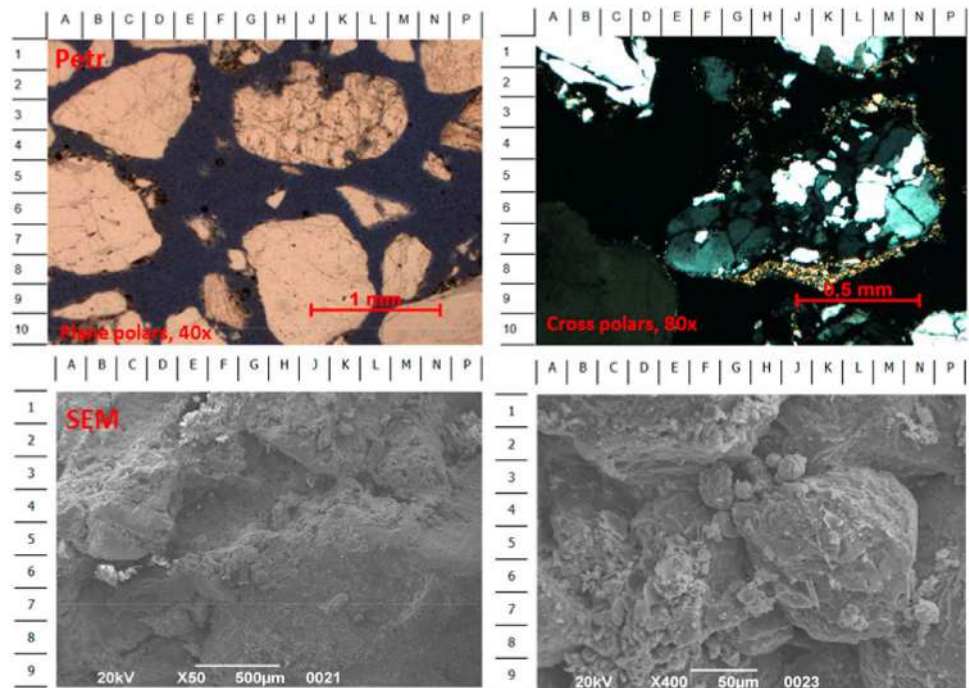
**Table 3** (continued)

FU7	Very fine-grained Sd, sub-ang-sub-rnd, moderate to good sorting. Planar & point contacts. Monocrystalline quartz, fresh & weathered K-feldspar, plagioclase, rock fragments (clay and chert), & low-grade metamorphic rock fragments. Minor glauconite, carbonaceous material, mica, and heavy minerals. Detrital clay and pseudomatrix. Diagenetic processes moderate compaction, elongated & point contacts, minor silica cementation, clay minerals, & siderite. Grain replacement by kaolinite, calcite, & pseudomatrix by siderite,	
	Dissolution, intergranular & microintercrystalline porosity	
FU8	Very fine-grained sandstone, sub-angular to sub-rounded, moderate sorting. Point contacts, planar & concave-convex contacts. Monocrystalline quartz, associated with feldspar, potassium feldspar, plagioclase, and microcline. Rock fragments polycrystalline quartz, chert, opaque minerals, gypsum, mica, and heavy minerals. Planktonic & benthic foraminifera, as well as miliolids. Compaction & partial replacement by siderite, pyrite, calcite, & clay minerals. Mainly intergranular porosity	
FU9	Fine-grained Sd, well-sorted, sub-angular to sub-rounded. Linear & concave-convex, quartz grains, rock fragments, primarily sedimentary and metamorphic, few volcanic fragments. Feldspar, mainly plagioclase, carbon fibers, mica, heavy minerals, & opaque minerals, matrix consists of detrital clay & pseudomatrix, cementation by silica, kaolinite, illite, & unidentified clays, generally grow within pore spaces. Replaced by kaolinite, authigenic clay, and pyrite. Feldspar, rock fragments, mica, and carbonaceous material, mechanical and chemical compaction plays a very dominant role, intergranular porosity, dissolution secondary porosity.	
FU10	Very fine-grained Sd, sub-angular to sub-rounded, moderate sorting, elongated & point contacts. Monocrystalline quartz, K-feldspar, plagioclase, & microcline. Accessory minerals mica, carbon grains, & heavy minerals. Detrital clay & thin clay laminations. Compaction, minor cementation by clay minerals, pyrite, silica, and siderite. Intergranular pore spaces are filled & matrix and grains are replaced by clay minerals, pyrite, and siderite, as well as dissolution. Interparticle & dissolution porosity.	

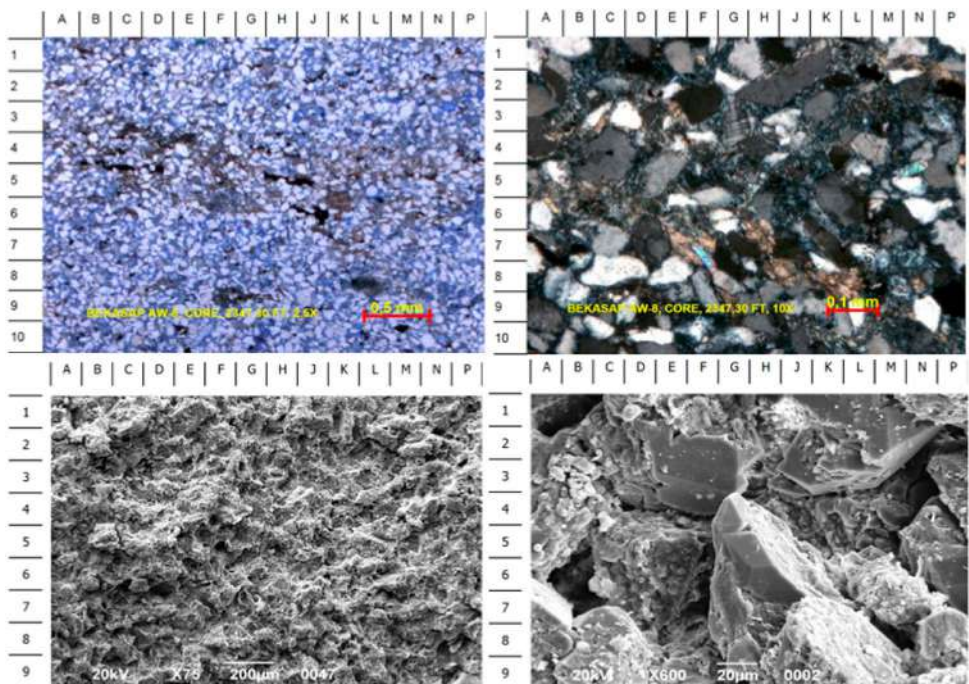
rock group is expected to have its own distinct quality. In sandstone, rock texture is the main factor determining rock quality (Amaefule et al. 1993). Also, Texture is a dominant factor influencing the saturation exponent and cementation exponent (Acosta et al. 2021). The saturation exponent is higher in samples with unconnected pores and greater hydraulic unit complexity. In contrast, it tends to decrease in rock samples with connected pores, which are characterized by lower hydraulic unit complexity (Saadat et al. 2024). A plot of the resistivity index against water saturation shows a shift in slope moving to the right for lower rock quality or

higher FU (Fig. 4). The same pattern is shown in the plot of formation factor against porosity (Fig. 5). The slope on the resistivity index plot against water saturation indicates that the saturation exponent increases as rock quality decreases. This proves a strong relationship between the global hydraulic element and the saturation exponent (Corbett and Mousa 2010). The plot of formation factor against porosity also shows a similar pattern, where the slope increases as rock quality decreases. The cementation factor varies depending on the lithology, particularly in relation to the clay content and its types (Wan Bakar et al. 2022) as well as

**Fig. 2** Petrographic analysis of rock samples for FU 1 (best quality rock group)



**Fig. 3** Petrographic analysis of rock samples for FU 10 (The worst quality rock group)



porosity types in carbonate rocks (Rostami et al. 2024). Shi-Jun demonstrated the impact of sandstone pore texture on the saturation exponent and cementation exponent (Shi-jun 2009). Several studies also indicate that the estimation of the saturation exponent ( $n$ ) and cementation exponent ( $m$ ) are influenced by rock quality (Jumaah 2021). By classifying rocks based on rock class determined by porosity, the saturation and cementation exponents can be well estimated (Venkataramanan et al. 2016).

### The influence of physical properties of rocks on rock quality and saturation exponent

The quality of rock is highly influenced by pore complexity. This pore complexity greatly determines the key physical properties of reservoir rock, such as porosity and permeability. As previously discussed, a group of rocks with the same quality exhibits similarities in shape factor and tortuosity (Amaefule et al. 1993). What differentiates them is the size

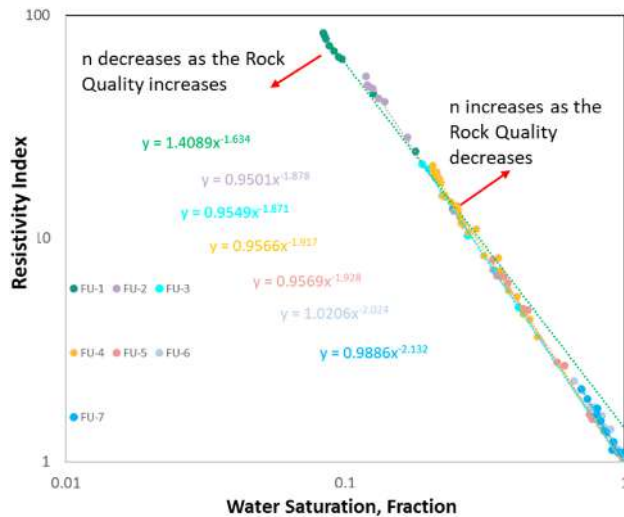


Fig. 4 Relationship between rock quality and saturation exponent

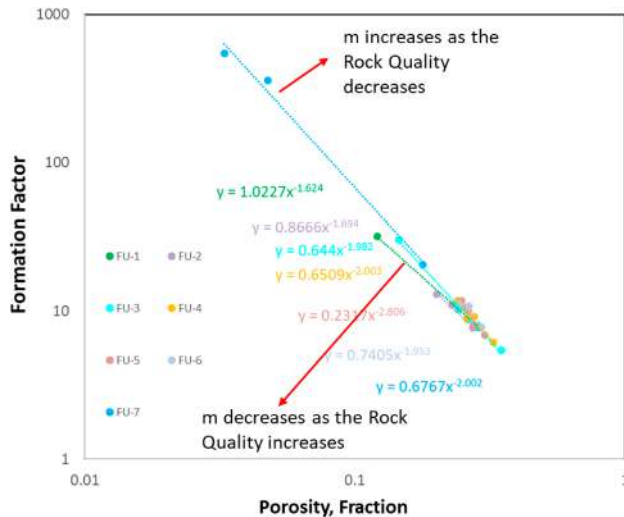


Fig. 5 Relationship between rock quality and cementation exponent

of the pore space, which is expressed as the mean hydraulic radius ( $RQI$ ). Thus, a group of rocks with the same quality should have the similar ability to transmit fluids. The ability a rock to transmit fluids is known as permeability. If permeability is influenced by pore complexity, then permeability should have an effect on the saturation exponent. Figure 6. shows the relationship between the saturation exponent and permeability, overlaid with Flow Unit (FU). Although not clearly visible, there is a certain trend of decreasing permeability with increasing saturation exponent.

Clay volume is one of the physical properties of rock that affects pore complexity. The presence of clay minerals in pore spaces varies between different types of clay. Illite and Smectite are types of clay that significantly influence pore complexity. These two minerals have a large specific surface area and a high cation exchange capacity (CEC).

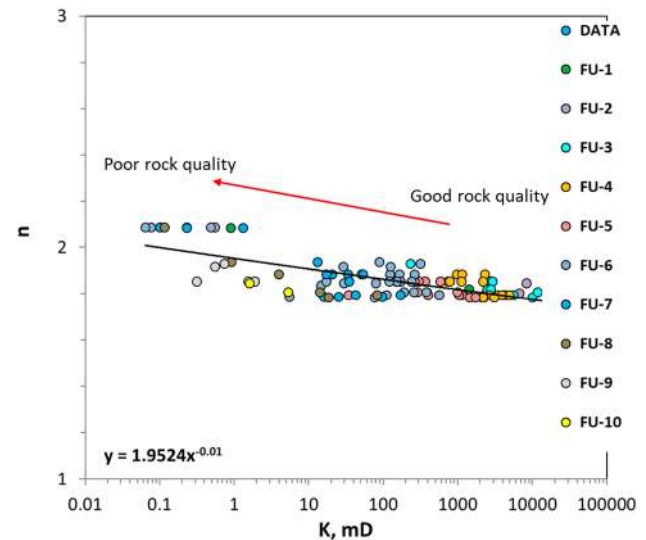


Fig. 6 Effect of permeability and rock quality on saturation exponent

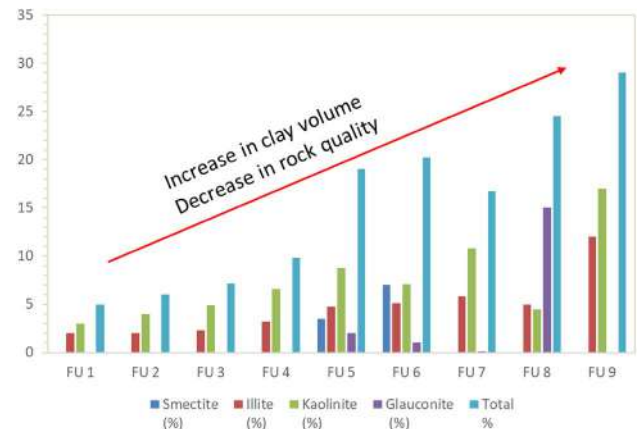
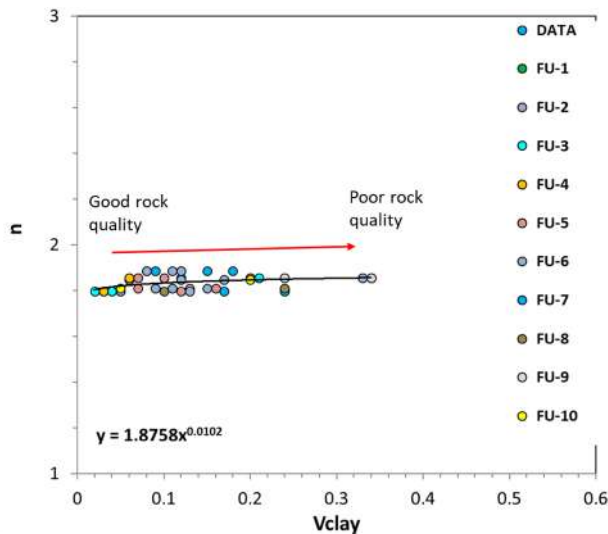


Fig. 7 Effect of clay volume on rock quality

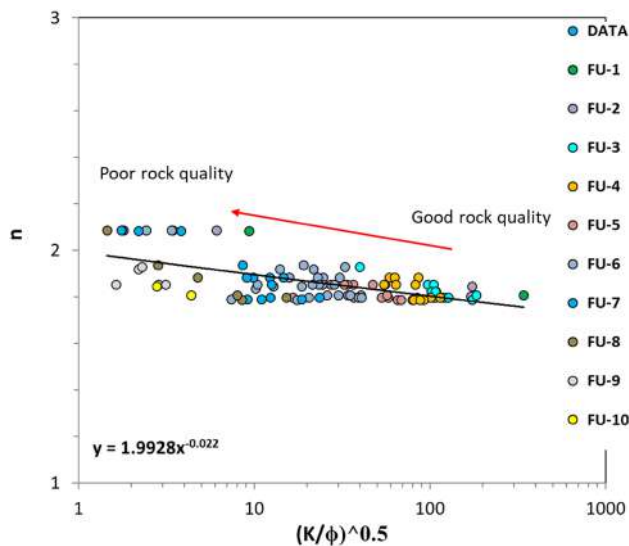
Figure 7. shows that clay volume has a significant impact on rock quality. An increase in clay volume leads to a decrease in rock quality.

The influence of clay volume on the saturation exponent is shown in Fig. 8. An increase in clay volume leads to a decrease in rock quality and an increase in the saturation exponent. Yufei Fan demonstrated that clay volume has a significant effect on the saturation exponent (Fan et al. 2020). Figure 7. shows that clay minerals are dominated by illite and kaolinite. Lower quality rock group (larger numbers of FU), the presence of illite, glauconite, and smectite is observed to decrease rock quality. This indicates that the presence of these three minerals increases pore complexity, resulting in a higher saturation exponent. The high cation exchange capacity (CEC) of illite and smectite also contributes to the increase in the saturation exponent (Kurniawan and Bassiouni 2007).





**Fig. 8** Effect of clay volume on saturation exponent



**Fig. 9** Effect of pore geometry on saturation exponent

### Relationship of reservoir quality index and saturation exponent

Amaefule defined the reservoir quality index (*RQI*) using the petrophysical properties of rock porosity and permeability, expressed as  $(k/\phi)^{0.5}$  (Amaefule et al. 1993). Wibowo referred to  $(k/\phi)^{0.5}$  as pore geometry, which is comparable to the mean hydraulic radius (Wibowo and Permadi 2015). This pore geometry involves the shape and size of the pores, thereby affecting pore volume. Good quality rocks group tend to have simple pore geometry or a larger mean hydraulic radius (Prakoso et al. 2021). Pore geometry is one of the factors that causes variations in the saturation exponent (Stalheim and Eidesmo 1995; Watfa 1991). Simple geometry with larger pore size tends to indicate better quality

and generally corresponds to a lower saturation exponent (Fig. 9). On the other hand, increasingly complexity of pore geometry indicates an increase in the saturation exponent.

### Relationship of specific surface area, Kozeny constant and saturation exponent

Specific surface area is the area of the pore space wetted by fluid relative to the pore volume. Specific surface area can be approximated using the Kozeny equation (Kozeny 1927). The Kozeny equation can be rearranged as follows:

$$K = 0.9869 \frac{C\phi^3}{S_b^2} \quad (9)$$

Equation 9 can be rearranged to estimate the specific surface area per unit bulk volume as follows:

$$S_b = \left( \frac{C\phi^3}{K/0.9869} \right)^{0.5} \quad (10)$$

$c$  is known as the Kozeny constant. The Kozeny constant is a function of the shape factor ( $F_s$ ) and tortuosity ( $\tau$ ) (Amaefule et al. 1993). Several studies have shown that shape factor ( $F_s$ ) and tortuosity ( $\tau$ ) are two factors that influence pore complexity. The shape factor affects the shape of pores, with a value of 1 for perfectly round pores, and increases as the pore shape becomes more complex. Tortuosity ( $\tau$ ) is a parameter that also reflects pore space complexity. The more complex of the pore space, the longer of the fluid flow paths. Thus, as pore space complexity increases, tortuosity ( $\tau$ ) also increases. The Kozeny constant ( $c$ ) can be approximated using the Mortensen equation (Mortensen et al. 2007). The Mortensen equation can be expressed as follows:

$$c = \left( 4 \cos \left( \frac{1}{3} \arccos \left( \phi \frac{8^2}{\pi^3} - 1 \right) + \frac{4}{3} \pi \right) + 4 \right)^{-1} \quad (11)$$

The influence of specific surface area on rock quality and the saturation exponent is shown in Fig. 10. Rocks with good quality tend to have a low specific surface area. This is due to the simple pore shape, which is nearly perfectly round, causing the shape factor to approach 1. Simple and interconnected pore spaces result in shorter fluid flow paths and a lower tortuosity factor.

Figure 11 provides information about the influence of the Kozeny constant on saturation exponent. A low Kozeny constant characterizes by a group of rocks with simple pore shapes, resulting in a low shape factor and low tortuosity, which indicates good quality. Zhang showed that low tortuosity contributes to a decrease in the saturation exponent (Zhang et al. 2021). Figure 11 proves that the Kozeny

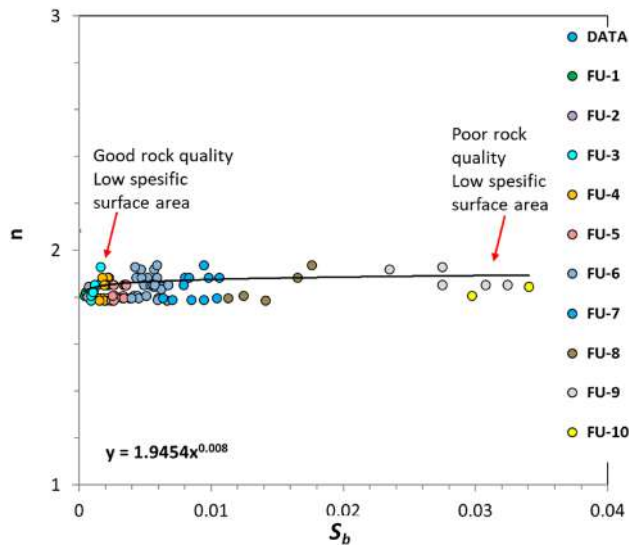


Fig. 10 Effect of specific surface area on saturation exponent

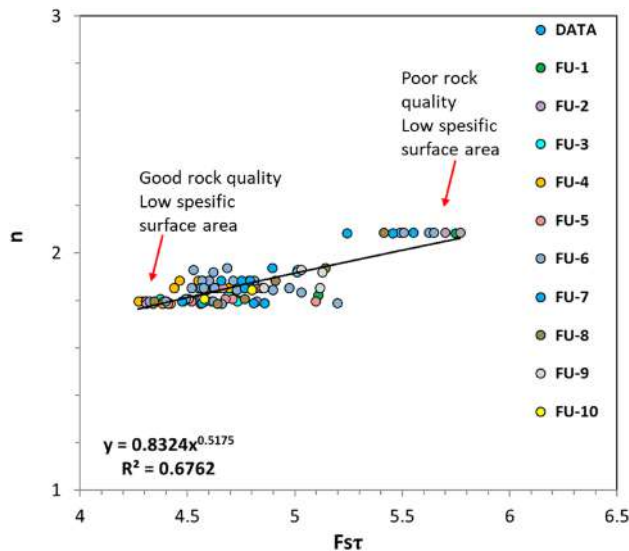


Fig. 11 Effect of Kozeny constant on saturation exponent

constant can provide an overview of rock quality and affects the saturation exponent. Good rock quality is characterized by a low Kozeny constant value and a low saturation exponent.

### Saturation exponent and water saturation estimation

Based on the previous discussion, it was found that the saturation exponent is significantly influenced by the combination of pore attributes that are shape factor and tortuosity, known as the Kozeny constant, and the physical properties of rock, specifically clay volume. A multivariate regression between the saturation exponent, Kozeny constant, and clay volume was established to obtain an empirical relationship

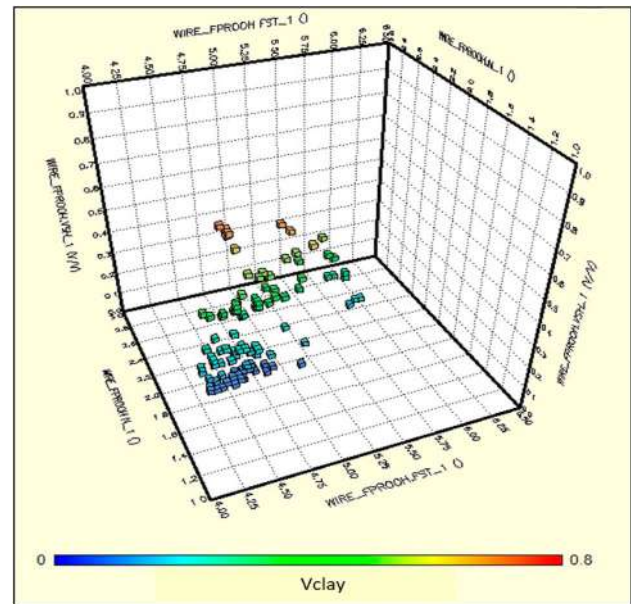


Fig. 12 Relationship between saturation exponent, Kozeny constant and clay volume

among these three parameters (Fig. 12). Based on the relationship of these three parameters, an empirical equation was derived to calculate the saturation exponent as follows:

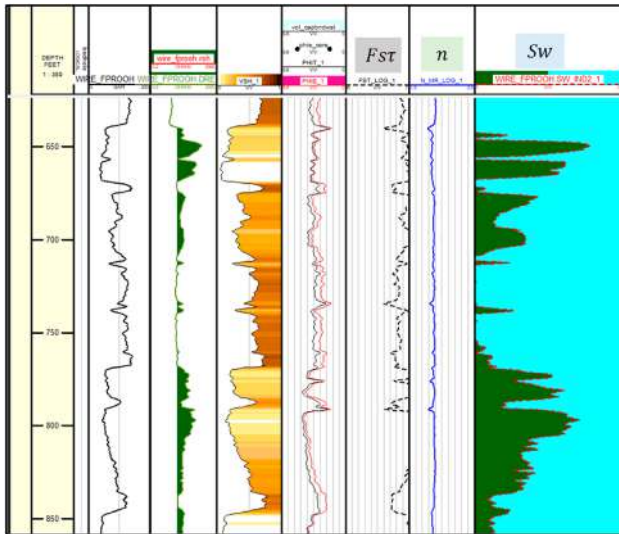
$$n = A + (B * F_s \tau) + (C * V_{clay}) \quad (12)$$

Where  $A$ ,  $B$ , and  $C$  are empirical constants for the Kozeny constant and clay volume, whose values may vary for each field. This study obtained the constant value  $A = 0.579697$ ,  $B = 0.180011$ , and  $C = 0.126903$ . Based on Eq. 12, the saturation exponent for entire depth interval can be estimated using porosity and clay volume (Fig. 13). While the porosity and clay volume were obtained from log analysis. The log curve of the saturation exponent ( $n$ ) obtained allows for an accurate calculation of water saturation (Fig. 13). These results demonstrate that integrating porosity and clay volume data from log analyses produces a consistent and accurate estimation of water saturation for entire depth interval.

### Result validation

Validation was performed by comparing the calculated water saturation with the water saturation data from the core (Figs. 14, 15 and 16). The water saturation estimated using the varying saturation exponent value yielded good results. Qualitatively, the calculated saturation results closely match the water saturation data from laboratory measurements (Figs. 14A, 15A and 16A). The plot comparing measured and calculated water saturation, although still somewhat scattered, shows a trend that follows the line represented by the equation  $Y = X$  (Figs. 14B, 15B and 16B).





**Fig. 13** Results of estimating the saturation exponent and water saturation calculation

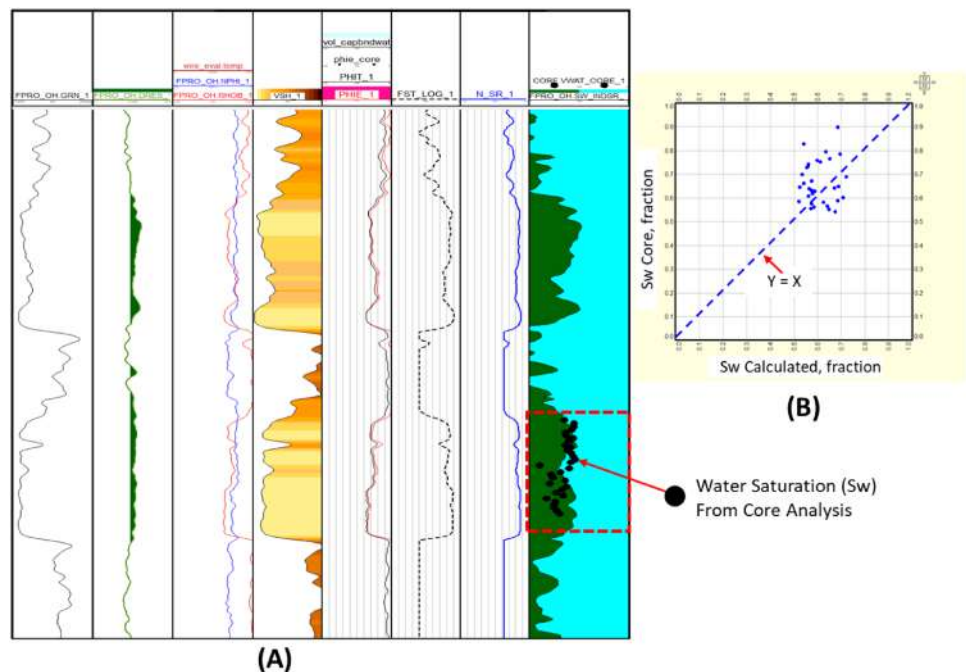
These results show that this study provides additional knowledge to the understanding of the relationship between pore quality and saturation exponent in water saturation calculations, especially in heterogeneous reservoir rocks. The findings show that the saturation exponent is not only influenced by the type of lithology, but also by the pore complexity. The approach of varying saturation exponent values for the entire reservoir can produce more accurate water saturation calculations. This study adds new understanding and a simple approach in estimating the saturation exponent required for water saturation calculations.

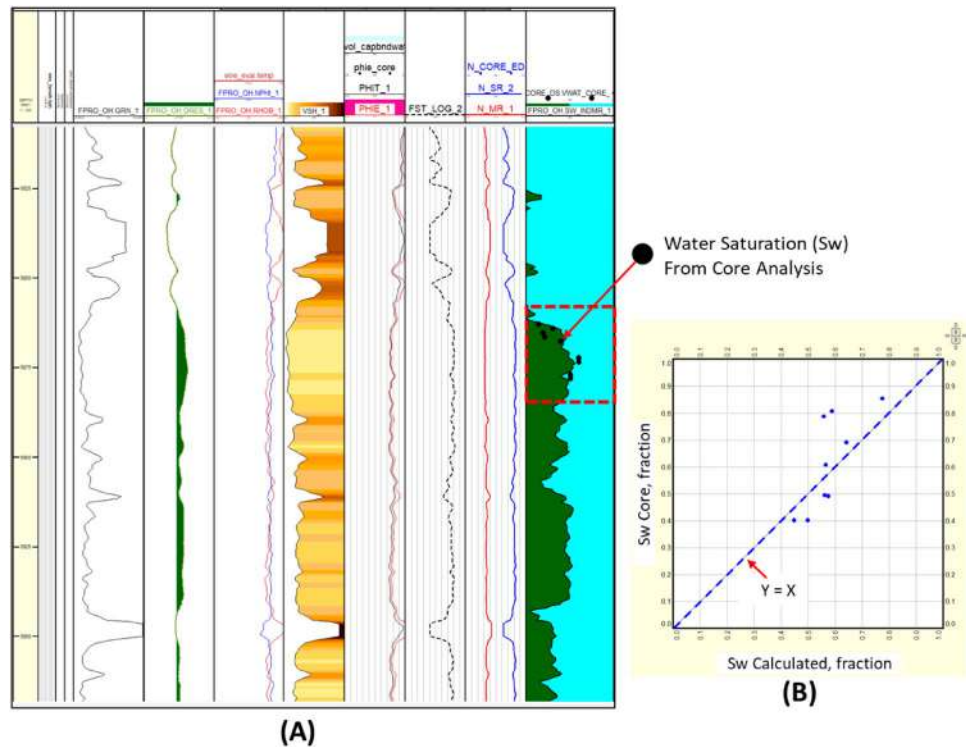
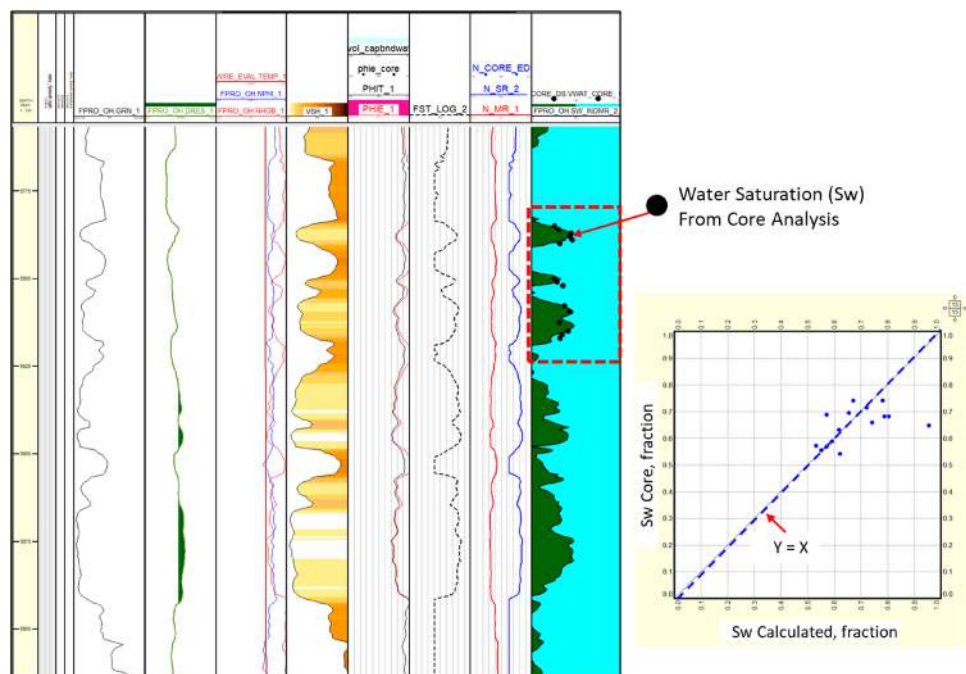
## Conclusions

Some conclusions obtained from this study are as follows:

1. In sandstone, the study of factors affecting rock quality (texture, porosity, and clay volume) revealed a negative relationship with the saturation exponent. The saturation exponent is lower for good rock quality, and a decrease in rock quality leads to an increase in the saturation exponent.
2. Flow unit-based observations show that the saturation exponent value increases with increasing flow unit numbers, indicating increasing pore complexity and decreasing rock quality. This decreasing rock quality is also shown in the relationship between permeability and clay volume with the saturation exponent, where decreasing permeability and increasing clay volume will increase the saturation exponent.
3. The reservoir quality index is an indicator of rock quality. The saturation exponent tends to be higher for rocks with a low reservoir quality index. The reservoir quality index is defined as a function of the pore shape factor and tortuosity.
4. The combination of the pore shape factor and tortuosity is widely known as the Kozeny constant. Considering that clay volume is one of the factors affecting rock quality, an empirical equation between the combination of pore shape factors and tortuosity attributes and clay volume with saturation exponent can be arranged.
5. The saturation exponent for the entire depth interval can be predicted well using the empirical equation obtained

**Fig. 14** Validation of water saturation calculation results of well A



**Fig. 15** Validation of water saturation calculation results of well B**Fig. 16** Validation of water saturation calculation results of well C

from this study (Eq. 12). The combination of pore shape factor and tortuosity can be calculated from porosity, while porosity and clay volume can be easily obtained from log analysis.

**Acknowledgements** We would like to thank the Ministry of Education, Culture, Research and Technology, LLDIKTI III and Institution of Research and Community Services Universitas Trisakti for their valuable support and assistance in this study. We are also grateful to

the optical petrography and mineralogy laboratory and core analysis laboratory, Faculty of Earth and Energy Technology for provided petrography analysis and core analysis data for this research work.

**Funding** This research was funded by the Indonesian Ministry of Education, Culture, Research and Technology, LLDIKTI III (2024) through competitive research grant under the Fundamental Research Scheme, contract number 832/LL3/AL.04/2024 & 180/A/LPPM-P/USAKTINI/2024. We appreciate for the financial support from these funding agencies.

## Declarations

**Conflict of interest** On behalf of all the co-authors, the corresponding author states that there is no conflict of interest.

**Open Access** This article is licensed under a Creative Commons Attribution-NonCommercial-NoDerivatives 4.0 International License, which permits any non-commercial use, sharing, distribution and reproduction in any medium or format, as long as you give appropriate credit to the original author(s) and the source, provide a link to the Creative Commons licence, and indicate if you modified the licensed material. You do not have permission under this licence to share adapted material derived from this article or parts of it. The images or other third party material in this article are included in the article's Creative Commons licence, unless indicated otherwise in a credit line to the material. If material is not included in the article's Creative Commons licence and your intended use is not permitted by statutory regulation or exceeds the permitted use, you will need to obtain permission directly from the copyright holder. To view a copy of this licence, visit <http://creativecommons.org/licenses/by-nc-nd/4.0/>.

## References

- Abu-Hashish MF, Afify HM (2022) Effect of petrography and diagenesis on the sandstone reservoir quality: a case study of the middle miocene Kareem formation in the North geisum oil field, Gulf of sues, Egypt. *Arab J Geosci* 15(6):465. <https://doi.org/10.1007/s12517-022-09686-z>
- Abu-Hashish MF, Ali SB (2021) Integration of well logs and seismic data for facies analysis and modelling of the El-Wastani Formation in the Sequoia Gas Field, offshore Nile Delta, Egypt. *J Afr Earth Sci*. <https://doi.org/10.1016/j.jafrearsci.2021.104343>
- Abu-Hashish MF, Al-Sharif AW, Hassan NM (2022) Hydraulic flow units and reservoir characterization of the Messinian Abu Madi Formation in West El Manzala Development Lease, onshore Nile Delta, Egypt. *J Afr Earth Sc*. <https://doi.org/10.1016/j.jafrearsci.2022.104498>
- Acosta ER, Nandlal B, Harripersad R (2021) Saturation exponent as a function of reservoir heterogeneity and wettability in the Tambaredjo Oil Field, Suriname. SPWLA 62nd Annual Online Symposium Transactions. <https://doi.org/10.30632/SPWLA-2021-0118>
- Adisoemarta PS, Anderson GA, Frailey SM, Asquith GB (2001) Saturation exponent  $n$  in well log interpretation: another look at the permissible range. *Soc Petroleum Eng - SPE Permian Basin Oil Gas Recovery Conf 2001 OGR 2001*. <https://doi.org/10.2118/70043-ms>
- Al-Dujaili AN (2023) Reservoir rock typing and storage capacity of Mishrif carbonate formation in West Qurna/1 Oil Field, Iraq. *Carbonates Evaporites*. <https://doi.org/10.1007/s13146-023-00908-3>
- Al-Dujaili AN, Shabani M, AL-Jawad MS (2021) Characterization of flow units, rock and pore types for Mishrif Reservoir in West Qurna oilfield, Southern Iraq by using lithofacies data. *J Petroleum Explor Prod Technol*. <https://doi.org/10.1007/s13202-021-01298-9>
- AL-Dujaili AN, Shabani M, AL-Jawad MS (2023) Effect of heterogeneity on capillary pressure and relative permeability curves in carbonate reservoirs. A case study for Mishrif formation in West Qurna/1 Oilfield, Iraq. *Iraqi J Chem Petroleum Eng*. <https://doi.org/10.31699/ijcpe.2023.1.3>
- Al-Hilali MM, Al-Abideen MJZ, Adegbola F, Li W, Avedisian AM (2015) A petrophysical technique to estimate archie saturation exponent ( $n$ ); Case studies in carbonate and shaly-sand reservoirs - IRAQI oil fields. *Society of Petroleum Engineers - SPE Annual Caspian Technical Conference and Exhibition, CTCE 2015*. <https://doi.org/10.2118/177331-ms>
- Al-Otaibi MH, Khamatdinov R, Al-Khalidi N, Abdelrahman R, Bouaouaja M (2012) Water saturation modeling in Khafji carbonate reservoir. *Society of Petroleum Engineers - Abu Dhabi International Petroleum Exhibition and Conference 2012, ADIPEC 2012 - Sustainable Energy Growth: People, Responsibility, and Innovation, 2*. <https://doi.org/10.2118/161427-ms>
- Amaefule JO, Altunbay M, Tiab D, Kersey DG, Keelan DK (1993) Enhanced reservoir description: using core and log data to identify hydraulic (Flow) units and predict permeability in uncored intervals/Wells. *SPE Annual Tech Conf Exhib*. <https://doi.org/10.2118/26436-MS>
- Ara TS, Talabani S, Atlas B, Vaziri HH, Islam MR (2001) In-depth investigation of the validity of the archie equation in carbonate rocks. *Proceedings-SPE production operations symposium*. <https://doi.org/10.2118/67204-ms>
- Archie GE (1942) The electrical resistivity log as an aid in determining some reservoir characteristics. *SPE Reprint Series*. <https://doi.org/10.2118/942054-g>
- Chen X, Kuang LC, Sun ZC (2002) Archie parameter determination by analysis of saturation data. *Petrophysics*, 43(2)
- Corbett PWM, Mousa NIA (2010) Petrotype-based sampling applied in a saturation exponent screening study, Nubian sandstone formation, Sirt basin, Libya. *Petrophysics*, 51(4)
- Donaldson EC, Siddiqui TK (1989) Relationship between the Archie saturation exponent and wettability. *SPE Form Eval*. <https://doi.org/10.2118/16790-pa>
- El-Khatib N (1995) Development of a modified capillary pressure J-Function. *Spe*, 547–562
- Fan Y, Pan B, Guo Y, Lei J (2020) Effects of clay minerals and Pore-Water conductivity on saturation exponent of clay-bearing sandstones based on digital rock. *Petrophys-SPWLA J Format Eval Reserv Descr* 61(04):352–362. <https://doi.org/10.30632/PJV61N4-2020a2>
- Hamada GM, AL-Awad MN, Alsughayer A (2002) Variable saturation exponent effect on the determination of hydrocarbon saturation. *All Days*. <https://doi.org/10.2118/77887-MS>
- Jumaah HA (2021) Modified Archie's parameters for estimating water saturation for carbonate reservoir in north of Iraq. *J Petroleum Explor Prod Technol*. <https://doi.org/10.1007/s13202-021-01258-3>
- Kozeny J (1927) Über kapillare Leitung des wassers Im Boden. *Akad Wiss Wien* 136:271–306
- Kumar M, Senden TJ, Sheppard AP, Arns CH, Knackstedt MA (2010) Variations in the archie's exponent: Probing wettability and low sw effects. *SPWLA 51st annual logging symposium 2010*
- Kurniawan B, Bassiouni Z (2007) Use of cec-dependent cementation and saturation exponents in shaly sand resistivity models. *48th annual logging symposium 2007*
- Mortensen J, Engstrom F, Lind I (2007) The relation among porosity, permeability, and specific surface of chalk from the gorm field, Danish North sea. *SPE Reservoir Eval Eng*. <https://doi.org/10.2118/31062-pa>
- Olusola BK, Aguilera R (2013) How to estimate water saturation exponent in dual and triple porosity reservoirs with mixed wettability. *Society of petroleum engineers-SPE Canadian unconventional resources conference 2013-unconventional becoming conventional: lessons learned and new innovations, 2*. <https://doi.org/10.2118/167213-ms>
- Prakoso S, Burhannudinnur M, Irham S, Rahmawan S, Yasmaniar G (2021) Linkage of cementation factor on rock quality in sandstone. *AIP Conf Proc*. <https://doi.org/10.1063/5.0061148>
- Rabiee R, Hamada G (2022) Artificial neural network modeling for water saturation determination in Shaly sandstone reservoirs:

- case study Egyptian oil field. SSRN Electron J. <https://api.semanticscholar.org/CorpusID:246988787>
- Rostami A, Helalizadeh A, Moghaddam MB, Soleymanzadeh A (2024) New insights into estimating the cementation exponent of the tight and deep carbonate pore systems via rigorous numerical strategies. *J Petroleum Explor Prod Technol* 14(6):1605–1629. <https://doi.org/10.1007/s13202-024-01776-w>
- Saadat K, Rahimpour-Bonab H, Tavakoli V, Gholinezhad J (2024) Experimental investigation and prediction of saturation exponent in carbonate rocks: the significance of rock-fluid properties. *J Petroleum Explor Prod Technol*. <https://doi.org/10.1007/s13202-023-01714-2>
- Shi-jun Y (2009) Influence of sandstone pore texture on cementation exponent and saturation error analysis in Kuche Area, Tarim Basin. *Well Logging Technology*. <https://api.semanticscholar.org/CorpusID:131019560>
- Sondena E, Brattell F, Kolltvelt K, Normann HP (1992) Comparison between capillary pressure data and saturation exponent obtained at ambient conditions and at reservoir conditions. *SPE Form Eval*. <https://doi.org/10.2118/19592-pa>
- Stalheim SO, Eidesmo T (1995) Is the saturation exponent  $n$  a constant? SPWLA 36th annual logging symposium 1995
- Tiab D, Donaldson EC (2015) *Petrophysics: theory and practice of measuring reservoir rock and fluid transport properties: Fourth Edition*. In *Petrophysics: theory and practice of measuring reservoir rock and fluid transport properties: Fourth Edition*. <https://doi.org/10.1016/C2014-0-03707-0>
- Tian J, Wang L, Rong Zhao R, Liu H, Qi Zhang Q, Sim H, Qiang L (2022) Improved triple porosity model for calculating porosity exponent of fractured-vuggy reservoirs based on Maxwell-Garnett mixing rule and anisotropic conductivity analysis. *J Petrol Sci Eng*. <https://doi.org/10.1016/j.petrol.2022.110265>
- Tian J, Wang L, Ostadhassan M, Zhang L, Liu H, Sima L (2024) Pore structure exponent of Archie's law in a dual-porosity medium: Vuggy reservoirs. *Geoenergy Sci Eng*. <https://doi.org/10.1016/j.geoen.2024.212659>
- Venkataramanan L, Donadille JM, Reeder SL, Van Steene M, Gkortsas VM, Fella K, Ramsdell D, Al-Rubaiyea JA, Al-Ajmi FA, Al-Houli M, Wilkinson P, Bajunaid H (2016) A new method to estimate cementation and saturation exponents from dielectric dispersion data. *Proc-SPE Annual Tech Conf Exhib*. <https://doi.org/10.2118/181451-ms>
- Wan Bakar WZ, Saaid M, Ahmad I, Amir MR, Japperi Z, Ahmad Fuad MFI (2022) Improved water saturation estimation in shaly sandstone through variable cementation factor. *J Petroleum Explor Prod Technol*. <https://doi.org/10.1007/s13202-021-01391-z>
- Watfa M (1991) Using electrical logs to obtain the saturation exponent ( $n$ ) in the Archie equation. *Proc Middle East Oil Show*. <https://doi.org/10.2523/21415-ms>
- Wibowo AS, Permadi P (2015) A type curve for carbonates rock typing. <https://doi.org/10.2523/iptc-16663-ms>
- Worthington PF, Pallatt N (1990) Effect of variable saturation exponent upon the evaluation of hydrocarbon saturation. *Proc-SPE Annual Tech Conf Exhib Omega*. <https://doi.org/10.2118/20538-ms>
- Yadav L, Singh A, Dasgupta T (2017) Experimental basis for prediction of cementation, water saturation and bound water volume exponents with grain size variation in fresh water fluvial reservoirs
- Zhang Z, Liu L, Li C, Cai J, Ning F, Meng Q, Liu C (2021) Fractal analyses on saturation exponent in Archie's law for electrical properties of hydrate-bearing porous media. *J Petrol Sci Eng*. <https://doi.org/10.1016/j.petrol.2020.107642>

**Publisher's note** Springer Nature remains neutral with regard to jurisdictional claims in published maps and institutional affiliations.

# Suryo Prakoso

## Assessing pore quality impact on saturation exponent

 Artikel Ilmiah

---

### Document Details

Submission ID

trn:oid:::3618:109925778

Submission Date

Aug 28, 2025, 4:22 PM GMT+7

Download Date

Aug 28, 2025, 4:36 PM GMT+7

File Name

Assessing pore quality impact on saturation exponent.pdf

File Size

4.9 MB

15 Pages

7,674 Words

42,999 Characters



# 3% Overall Similarity

The combined total of all matches, including overlapping sources, for each database.





## Filtered from the Report

- Bibliography
- Quoted Text
- Small Matches (less than 15 words)




## Exclusions

- 14 Excluded Sources
- 5 Excluded Matches

## Match Groups

-  **9 Not Cited or Quoted 3%**  
Matches with neither in-text citation nor quotation marks
-  **0 Missing Quotations 0%**  
Matches that are still very similar to source material
-  **0 Missing Citation 0%**  
Matches that have quotation marks, but no in-text citation
-  **0 Cited and Quoted 0%**  
Matches with in-text citation present, but no quotation marks

## Top Sources

- 2%  Internet sources
- 3%  Publications
- 2%  Submitted works (Student Papers)

## Integrity Flags

0 Integrity Flags for Review

Our system's algorithms look deeply at a document for any inconsistencies that would set it apart from a normal submission. If we notice something strange, we flag it for you to review.

A Flag is not necessarily an indicator of a problem. However, we'd recommend you focus your attention there for further review.

## Match Groups

- 9** Not Cited or Quoted 3%  
Matches with neither in-text citation nor quotation marks
- 0** Missing Quotations 0%  
Matches that are still very similar to source material
- 0** Missing Citation 0%  
Matches that have quotation marks, but no in-text citation
- 0** Cited and Quoted 0%  
Matches with in-text citation present, but no quotation marks

## Top Sources

- 2% Internet sources
- 3% Publications
- 2% Submitted works (Student Papers)

## Top Sources

The sources with the highest number of matches within the submission. Overlapping sources will not be displayed.

- 1

Internet

www.karyailmiah.trisakti.ac.id

<1%
- 2

Student papers

University of Trinidad and Tobago on 2018-03-06

<1%
- 3

Internet

unsworks.unsw.edu.au

<1%
- 4

Publication

Mojtaba Homaie, Ida Lykke Fabricius, Morten Leth Hjuler, Asadollah Mahboubi, A...

<1%
- 5

Internet

ijcpe.uobaghdad.edu.iq

<1%
- 6

Student papers

Curtin University of Technology on 2017-11-13

<1%
- 7

Student papers

Colorado School of Mines on 2010-12-14

<1%
- 8

Internet

www.tandfonline.com

<1%

## ORIGINAL PAPER - PRODUCTION ENGINEERING



# Assessing pore quality impact on saturation exponent and water saturation calculation

Suryo Prakoso<sup>1</sup> · Muhammad Burhannuddinur<sup>2</sup> · Firman Herdiansyah<sup>2</sup> · Sigit Rahmawan<sup>1</sup> · Billy Arioseno Prakoso<sup>1</sup>

Received: 22 September 2024 / Accepted: 9 June 2025  
 © The Author(s) 2025

## Abstract

The saturation exponent is one of the most important parameters needed to calculate water saturation in Archie's equation. Generally, the saturation exponent is considered constant, but not all depth intervals have the same characteristics. This study aims to investigate the relationship between rock quality and the saturation exponent, a critical parameter in Archie's equation for water saturation calculation. Given that rock texture and pore characteristics vary significantly with depth, assuming a constant saturation exponent can lead to inaccurate results. The study integrates core analysis and petrographic data to classify rock quality and its relationship with the saturation exponent.  $R_i$  and  $R_o$  data from core analysis are used to determine saturation exponent. Furthermore, rock quality is identified using the hydraulic flow unit concept by constructing log-log plots of reservoir quality index and pore volume to grain volume ratio. Several pore attribute parameters, such as the combination of shape factor and tortuosity (Kozeny's constant), specific surface area, reservoir quality index, and clay volume, are examined for their influence on the saturation exponent. The saturation exponent shows strong correlation with Kozeny's constant and clay volume. An empirical equation was developed to estimate the saturation exponent based on these parameters. Using this empirical equation, the saturation exponent can be estimated across depth intervals, leading to more accurate water saturation calculations. This study offers a practical method to estimate saturation exponent variation using readily available log-derived parameters. It contributes to more reliable determination of saturation exponent variation and enhances the accuracy of water saturation calculations in heterogeneous formations.

**Keywords** Konzeny constant · Saturation exponent · Shape factor · Tortuosity · Reservoir quality index

## Nomenclatures

### Latin letters

$a$	Tortuosity factor
$c$	Kozeny constant
$m$	Cementation exponent
$n$	Saturation exponent
$A$	Empirical constants
$B$	Empirical constants
$C$	Empirical constants
$F$	Formation factor

$F_s$	Shape factor
$K$	Permeability, mD
$R_o$	Rock resistivity filled 100% water, Ohm-m
$R_t$	Measured rock resistivity, Ohm-m
$R_w$	Water resistivity, Ohm-m
$S_w$	Water saturation, fraction
$S_{vgr}$	Specific internal surface area per unit grain volume, cm-l or $\mu\text{m-l}$
$S_b$	Specific internal surface area per unit bulk volume, cm-l or $\mu\text{m-l}$
$T$	Tortuosity
$V_{clay}$	Volume clay, fraction

✉ Suryo Prakoso  
 suryo\_prakoso@trisakti.ac.id

<sup>1</sup> Petroleum Engineering, Faculty of Earth and Energy Technology, Universitas Trisakti, Jakarta, Indonesia

<sup>2</sup> Geological Engineering, Faculty of Earth and Energy Technology, Universitas Trisakti, Jakarta, Indonesia

## Greek letter

$\phi$	Porosity, fraction
$\phi_z$	Ratio of pore volume to grain volume

## Acronyms

CEC	Cation exchange capacity, meq/g
-----	---------------------------------

<i>FU</i>	Flow unit
<i>FZI</i>	Flow zone indicator
<i>RI</i>	Resistivity index
<i>RQI</i>	Reservoir quality index
<i>SCAL</i>	Special core analysis
<i>XRD</i>	X-ray diffraction

## Introduction

The saturation exponent ( $n$ ) is one of the most fundamental parameters for calculating water saturation using Archie's equation (Shi-jun 2009). If obtaining the saturation exponent ( $n$ ) from core measurements is not possible, it is typically assumed to be a constant value, usually 2. In most cases, the water saturation calculation for the entire depth interval is represented by a constant saturation exponent (Al-Otaibi et al. 2012). However, under certain conditions, assuming this constant value can lead to significant errors in the calculated water saturation.

In sandstone, the sedimentation process and depositional environment significantly influence the variability of the reservoir's physical properties and rock quality (Abu-Hashish et al. 2022; Abu-Hashish and Afify 2022; Abu-Hashish and Ali 2021). This variability indicates that the saturation exponent cannot be represented by a single constant value (Hamada et al. 2002; Yadav et al. 2017). In shaly sandstone, the clay volume fraction, as well as clay minerals with varying conductivity, show a significant effect on the saturation exponent (Fan et al. 2020; Kurniawan and Bassiouni 2007). The uncertainty in the saturation exponent ( $n$ ) may be caused by the complexity of pore geometry and pore type, structural heterogeneity, along with variations in wettability (Kumar et al. 2010).

Several factors can contribute to the saturation exponent uncertainty. Some studies suggest that the type of porosity not only affects the cementation factor ( $m$ ) but also the saturation exponent (Olusola and Aguilera 2013; Tian et al. 2022, 2024; Watfa 1991). Variations in the rock's microstructure, such as reservoir heterogeneity, wettability, and rock texture (Acosta et al. 2021; Adisoemarta et al. 2001), can influence the resistivity index and cause uncertainty in determining the saturation exponent. The presence of rock microstructure leads to pore complexity, characterized by pore geometry and structure, which affect pore space connectivity and wettability. Lower pore area and tortuosity contribute to a decrease in the saturation exponent (Zhang et al. 2021). Variations in the saturation exponent related to pore geometry effects can result in errors exceeding 10 saturation units in water saturation evaluation (Stalheim and Eidesmo 1995; Watfa 1991; Worthington and Pallatt 1990).

Changes in wettability conditions can affect fluid distribution within the pores space of rock, influencing resistivity response and complicating the estimation of the saturation exponent (AL-Dujaili et al. 2023; Donaldson and Siddiqui 1989). The rock's wettability preference has significant impacts on water saturation and saturation exponent (Sondena et al. 1992). The presence of authigenic clay increases oil-wet characteristics and affects the saturation exponent (Corbett and Mousa 2010; Rabiee and Hamada 2022; Shi-jun 2009).

Various methods have been used by researchers to determine the saturation exponent ( $n$ ), such as regression approaches involving water saturation and porosity (Hamada et al. 2002), and resistivity (Al-Hilali et al. 2015; Corbett and Mousa 2010). The saturation exponent describes how the rock's resistivity changes with varying water saturation (Adisoemarta et al. 2001; Olusola and Aguilera 2013; Venkataramanan et al. 2016). Differences in water saturation for heterogeneous reservoirs indicate changes in wettability, which are directly related to the saturation exponent (Adisoemarta et al. 2001). The change in wettability is linearly correlated with the change in the saturation exponent (Donaldson and Siddiqui 1989).

This study aims to determine the value of the saturation exponent by considering heterogeneity and differences in rock quality. The variation in the saturation exponent with respect to heterogeneity and differences in rock quality are not yet fully understood, creating the need for a more comprehensive approach that takes into account the parameters influencing rock quality. The integration of petrographic analysis, routine core analysis, and special core analysis data is used to develop a model that more comprehensively considers for this variability. The variable saturation exponent values obtained from this approach are expected to provide more accurate water saturation estimates in a simpler manner.

## Data and methods

### Data

This study uses sandstone data from the Central Sumatra Basin. The general lithological description consists of sandstone with grain sizes ranging from coarse to fine, with good to poor sorting, expected to represent the overall rock group. The research utilizes both routine core and *SCAL* data, including porosity, permeability, and resistivity index. The routine core data consists of porosity and permeability, while special core analysis (*SCAL*) data includes the formation factor and resistivity index. Sedimentological data, such as petrography (thin sections) and X-ray diffraction (*XRD*),

are also incorporated. The routine core data show variations in porosity and permeability (Table 1). The porosity data ranges from 4.5 to 36.9%, permeability data ranges from 0.12 to 33,400 mD, and clay volume is below 20%.

## Methods

### Formation resistivity factor and resistivity index

Archie formulated an equation to describe the resistivity behavior of reservoir rock based on core data measurements conducted in the laboratory (Archie 1942). Equation 1 determines the resistivity of rock that is fully saturated with formation water. The Formation Factor ( $F$ ) is defined as the ratio of the resistivity of rock that is 100% saturated with saline water to the resistivity of saline water  $R_w$ .

$$F = \frac{R_o}{R_w} = \frac{a}{\phi^m} \quad (1)$$

Archie's Eq. 2 describes the change in resistivity caused by hydrocarbon saturation. Archie defines the resistivity index,  $RI$ , as the ratio of the measured resistivity of the rock,  $R_t$ , to the resistivity of the rock when it is 100% saturated with formation water  $R_o$ .

$$RI = \frac{R_t}{R_o} = \frac{1}{S_w^n} \quad (2)$$

Where  $F$  is the Formation Factor,  $R_o$  is the resistivity of the rock 100% saturated with water,  $R_w$  is the water resistivity,  $\phi$  is the porosity,  $R_t$  is the true resistivity of the rock,  $S_w$  is the water saturation,  $a$  is the tortuosity factor,  $m$  is the cementation exponent, and  $n$  is the saturation exponent.

The ratio  $R_t/R_o$  is known as the resistivity index ( $RI$ ), which is primarily influenced by the salinity of the formation water (Tiab and Donaldson 2015). Although  $RI$  is generally considered to be unity at 100%  $S_w$ , many researchers have experimentally agreed that this value is not unity (Ara et al. 2001; Chen et al. 2002; Tiab and Donaldson 2015).

Equation 1 can be rearranged as follows:

$$\log F = \log a - m \log \phi \quad (3)$$

When the formation factor data is plotted against porosity on a log-log graph, drawing a line through the point (1,1)

and not through the point (1,1) produces a slope that represents the cementation exponent ( $m$ ).

Equation 2 can be rearranged as follows:

$$-n \log S_w = \log 1/I \quad (4)$$

On a log-log graph, plotting the resistivity index against saturation, drawing a line from the point (1,1) will produce a slope that represents the saturation exponent ( $n$ ).

### Rock quality grouping

Reservoir quality grouping is the process of characterizing reservoir rocks based on their dynamic behavior. The dynamic behavior of a group of rocks are determined by studying the complexity of the pore space through texture, rock fabric, diagenetic processes, and the interaction between the rock itself and the fluid (Al-Dujaili 2023). El-Khatib demonstrated that rock samples with similar capillary pressure curves should have the same tortuosity ( $\tau$ ) and irreducible water saturation ( $S_{wi}$ ) (El-Khatib 1995). Similarities in pore architecture are reflected by similarities in pore shape and tortuosity, where the combination of these two pore attributes are known as the Kozeny constant (Kozeny 1927). Amaefule rearranged the Kozeny equation as follows (Amaefule et al. 1993):

$$\left(\frac{K}{\phi}\right)^{0.5} = \frac{1}{S_{vgr} \sqrt{F_s \tau}} \left(\frac{\phi}{1-\phi}\right) \quad (5)$$

Where  $K$  is permeability,  $\phi$  is porosity,  $F_s$  is the shape factor,  $\tau$  is tortuosity, and  $S_{vgr}$  is the specific internal surface area.  $(k/\phi)^{0.5}$  describes the pore geometry, representing the mean hydraulic radius, which is known as the Reservoir Quality Index ( $RQI$ ), and  $\frac{1}{S_{vgr} \sqrt{F_s \tau}}$  represents the Flow Zone Indicator ( $FZI$ ). Equation 5 can be rearranged as follows:

$$RQI = FZI (\phi_z) \quad (6)$$

$\phi_z$  is the ratio of pore volume to grain volume as follows:

$$\phi_z = \left(\frac{\phi}{1-\phi}\right) \quad (7)$$

Equation 6 can be written in log-log form as follows:

$$\log RQI = \log FZI + \log (\phi_z) \quad (8)$$

Equation 8 produces a straight line on a log-log plot of  $RQI$  vs.  $\phi_z$ . The intercept of the straight line at  $\phi_z = 1$  represents the Flow Zone Indicator ( $FZI$ ). Samples with different  $FZI$  values will lie on parallel lines.  $FZI$  indicates similarity in

**Table 1** Data used in the study

Number of samples				Rock properties	
Routine	SCAL	Petrography	XRD	Porosity %	Permeability mD
Core					
104	104	45	45	4.5–36.9	0.12–33,400



pore throat characteristics, which corresponds to the flow unit. Rocks composed of fine grains and poor sorting tend to have a large surface area and high tortuosity, resulting in a low *FZI* value. Conversely, coarse-grained, non-shaly, and well-sorted rocks tend to have smaller surface areas and lower tortuosity, resulting in a higher *FZI* values (Al-Dujaili et al. 2021).

## Study's workflow

Table 2 outlines the research steps undertaken to achieve the objectives of this study. The first step involves obtaining the necessary data for the research. This data is acquired through laboratory measurements following standard rock analysis procedures, including selecting rock samples,

**Table 2** Research Steps

Step 1		Obtaining research data	
Rock Sample Selection	⇒	Number of Samples	⇒ Laboratory Analysis
Determine and select the representative sandstone samples that represent variations in depositional environment, stratigraphy, and mineralogy.		a. Determine the number of samples to be tested based on the research objectives and the required data. b. Ensure that the selected samples represent variations that describe heterogeneity.	Analyze the required parameters, namely lithology, texture and mineralogy through petrographic analysis. Measure the physical properties of rocks, namely porosity and permeability, Resistivity index and capillary pressure through routine core analysis and special core analysis.
Target Output		Obtaining representative research data to evaluate the saturation exponent parameters.	

Step 2		Conduct analysis and integrate data to obtain sufficient information to establish a relationship between rock quality and saturation exponent.	
Lithology and Texture Analysis	⇒	Rock Quality Identification	⇒ Determination of Saturation Exponent Parameters
Determine lithology, dominant texture and mineralogy and identify rock heterogeneity and quality.		Using porosity and permeability data to identify rock quality using the hydraulic flow unit concept.	Processing resistivity index data to obtain saturation exponent and analyzing the influence of petrophysical properties of rock on saturation exponent.
Target Output		Obtaining the most dominant factors influencing heterogeneity, reservoir quality and saturation exponent	

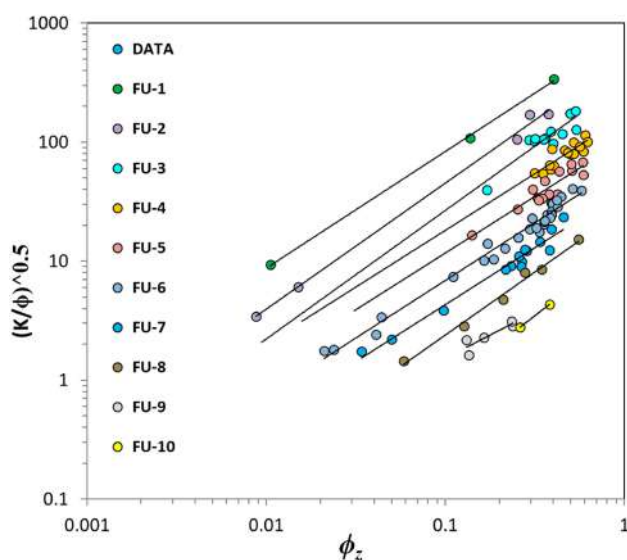
Step 3		Construct a model for estimating the saturation exponent from research findings.		
Data Integration and Analysis	⇒	Factors Affecting Rock Quality	⇒ The Effect of Rock Quality on Saturation Exponent	⇒ Saturation Exponent Estimation Approach
Obtain an understanding of the effect of heterogeneity on rock quality, as well as its implications for the saturation exponent.		Determining the most dominant factors that influence rock quality including porosity, permeability, clay volume, lithology, texture, pore geometry and internal pore characteristics such as pore shape factor and tortuosity.	Obtaining the relationship and influence of rock quality on the saturation exponent.	Developing an empirical equation for the saturation exponent.
Target Output		Obtaining a saturation exponent estimation approach.		

determining the number of samples, and defining the analysis protocols. The second step focuses on data analysis to establish the relationship between rock quality and the saturation exponent. This stage encompasses lithology and texture analysis, rock quality identification, and determining the saturation exponent. The final step involves developing an empirical equation to estimate the saturation exponent based on the research findings. These steps are designed to yield representative results for saturation exponent estimation and ensure accurate water saturation calculations.

## Results and discussion

### Rock quality identification

Rock quality is identified by the similarity of specific surface area, shape factor and tortuosity, known as the Flow Zone Indicator (*FZI*) (Amaefule et al. 1993). A plot between the reservoir quality index ( $((k/\phi)^{0.5})$ ) and the ratio of pore volume to grain volume can separate into several rock groups (Fig. 1). Rock samples can be classified into 10 rock groups based on their pore quality. FU 1 represents a group of rocks with the highest pore quality, while FU 10 represents group of rocks with low quality and high pore complexity. Each rock group shares similar specific surface area, pore shape ( $F_s$ ) and tortuosity. Figure 1 shows that although pore shape ( $F_s$ ) and tortuosity are similar, as the pore space increases, the value of  $(k/\phi)^{0.5}$  also increases.  $(k/\phi)^{0.5}$ , which is known as pore geometry (Wibowo and Permadi 2015), corresponds to the hydraulic pore radius (Kozeny 1927), so the difference within one rock group lies in varying pore sizes. This pore geometry is a characteristic of the pore space directly



**Fig. 1** Identification of rock quality based on the similarity of Flow Zone Indicators

related to rock quality and influences fluid flow (Amaefule et al. 1993; Wibowo and Permadi 2015).

Petrographic data is used to describe the microscopic geological features of each rock group. Table 3 provides an overview of the dominant factors influencing each rock group. Texture is the main factor that differentiates each rock group.

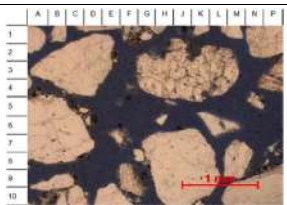

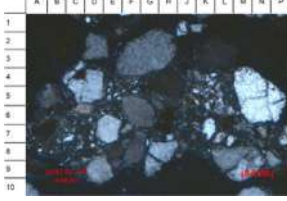
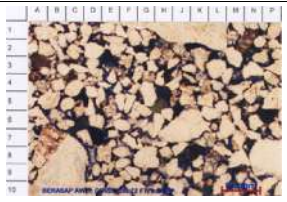
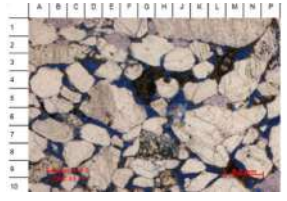
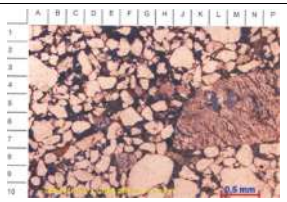
Figure 2 represents the results of petrographic analysis for the best quality of rock group. The petrographic analysis shows that the pore geometry exhibits a loose structure with coarse grains. The observed diagenesis includes pore-filling calcite, kaolinite, pore-lining illite, quartz overgrowth, and a small amount of pyrite. The dissolution of feldspar and matrix has developed into secondary porosity. Based on the SEM data, intensive quartz growth protects the rock from excessive compaction (low-degree compaction), thus preserving primary porosity. Authigenic pyrite partially covers the primary porosity, and kaolinite cement is present in pore spaces and pore channels, but this is minimal. With the development of matrix into secondary porosity and the preservation of primary porosity, this rock has relatively good porosity of 28.8% and permeability in the Darcy range.

Figure 3 represents the results of petrographic analysis for the poorest quality rock group. The petrographic analysis shows that the diagenetic process consists of cementation by quartz overgrowth, illite, kaolinite, and pyrite, followed by the alteration of most unstable grains and matrix into illite, kaolinite, and pyrite. The dissolution of unstable grains has formed secondary porosity. The compaction process, with moderate to high compaction levels, is evident from grain-to-grain contact, indicated by the presence of linear and concavo-convex contacts, as well as pseudo-matrix. The observed porosity in this rock group ranges from poor to moderate, consisting of intergranular porosity, secondary porosity from dissolution, and microporosity that develops between clay minerals. Generally, pore connectivity is poor due to the high content of clay matrix, cementation, and compaction. Pore sizes vary relatively from 2.5 to 60 microns, while microporosity has pore sizes ranging from 0.2 to 1 micron. Kaolinite fills the space between grains as cement. Compaction and cementation are the main factors controlling the decrease in the quality of rock group.

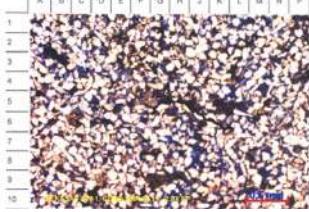
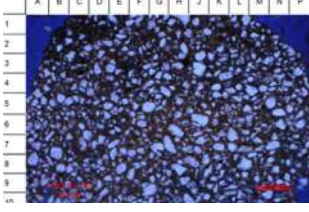
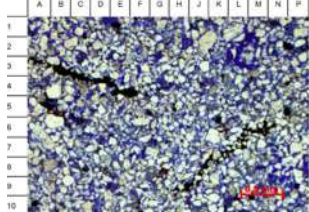

### Formation resistivity factor and resistivity index

The rock typing method is widely used to classify reservoir rocks into distinct groups based on their specific characteristics. Rocks within each group are deposited under similar geological conditions and undergo similar diagenetic processes. These groups share similarities in pore architecture, which can be identified through microscopic geological features (Wibowo and Permadi 2015). Therefore, each

**Table 3** Microscopic geological feature for each rock group

FU	Microscopic Description	Petrography
FU1	Coarse-grained Sd, mod. sorting, sub-angular to sub-rounded. The dominant mineral is quartz (88%), followed by feldspar (5%), metamorphic rock fragments (4.5%), a small amount of calcite cement and clay minerals	
FU2	Fine-medium-grained sandstone, sub-angular-rounded, poorly sorted. point contact with elongated types. Fragments consist of monocrystalline quartz, a small amount of polycrystalline quartz, microcline, and K-feldspar. Frag. clay (1%) and chert (0.5%). Accessory minerals mica, carbon matrix, and heavy minerals. A small amount of detrital clay matrix and pseudomatrix. Diag. Mod. compaction, point & long contacts. Intergranular & dissolution	
FU3	Loose Sd & Sd, Fine to med., poor to mod.srt, sub-ang. to sub-rnd, point contact, floating & planar. Main component is monocrystalline quartz, fragments polycrystalline quartz, metamorphic fragments, feldspar, and plagioclase. Opaque minerals, small amounts of mica, skeletal planktonic foraminifera, miliolids, small benthics, and detrital clay are also present. Diagenesis compaction, minor precipitation of pyrite within foraminifera chambers, and the replacement calcite, clay minerals & pyrite. Predominantly intergranular	
FU4	Fine to medium-textured Sd, sub-angular to sub-rounded, and moderate Srt. Long & concave-convex contacts. Primary grains are monocrystalline quartz, add. metamorphic and sedimentary frag. Microcline, orthoclase, mica & heavy minerals. Minor pseudomatrix & high-degree compaction. Silica overgrowth, along with kaolinite and siderite replacement. Dissolution secondary porosity.	
FU5	Med.-very coarse Sd, poorly sorted, sub-ang. to sub-rnd. Long & concave-convex Contact. Dominant monocrystalline quartz, add. feldspar (plagioclase and microcline). Minor benthic foraminifera & pseudo-matrix. Detrital clay & carbonate mud. Compaction is strong, with feldspar grain dissolution, minor pyrite precipitation, and clay minerals. Replacement siderite, pyrite, illite, dolomite, calcite, & kaolinite is observed. Intergranular, micro-pores, & dissolution porosity	
FU6	Med-very coarse grain Sd, sub-ang. to sub-rnd., poorly sorted, elongated grain contacts & point contacts. Main components monocrystalline quartz, K-feldspar, shale, silty shale, chert & plagioclase. Skeletal grains from benthic & planktonic foraminifera. Accessory minerals include mica and heavy minerals. Pseudo-matrix is also present, with dispersed distribution and thin laminations. Diagenetic compaction, siderite precipitation, slight replacement of the matrix by siderite, & dissolution. Intergranular & dissolution porosity.	

**Table 3** (continued)

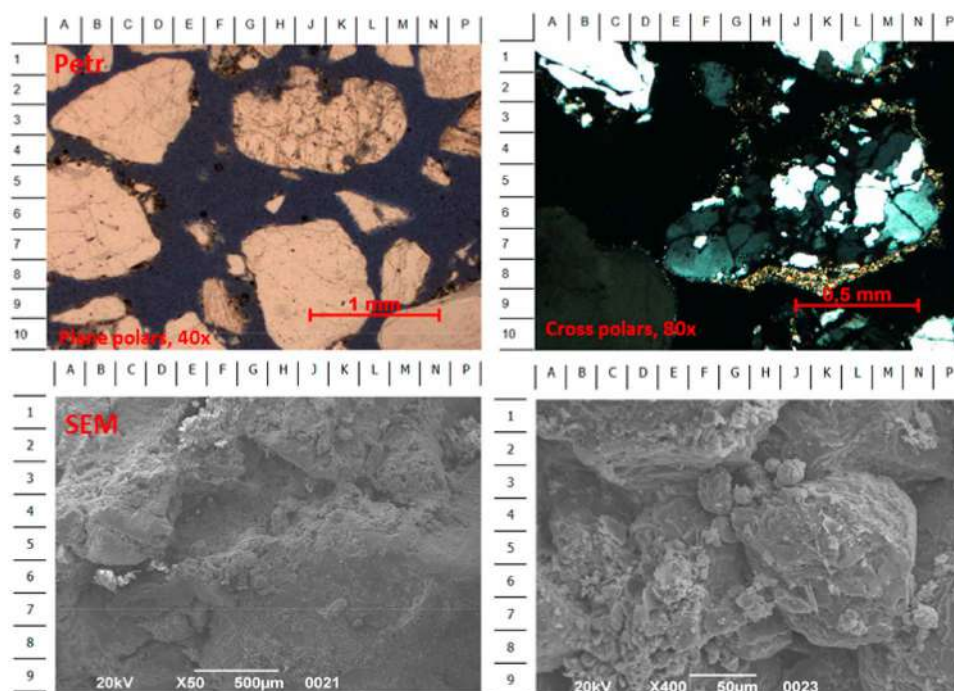
FU7	Very fine-grained Sd, sub-ang-sub-rnd, moderate to good sorting. Planar & point contacts. Monocrystalline quartz, fresh & weathered K-feldspar, plagioclase, rock fragments (clay and chert), & low-grade metamorphic rock fragments. Minor glauconite, carbonaceous material, mica, and heavy minerals. Detrital clay and pseudomatrix. Diagenetic processes moderate compaction, elongated & point contacts, minor silica cementation, clay minerals, & siderite. Grain replacement by kaolinite, calcite, & pseudomatrix by siderite,	
	Dissolution, intergranular & microintercrystalline porosity	
FU8	Very fine-grained sandstone, sub-angular to sub-rounded, moderate sorting. Point contacts, planar & concave-convex contacts. Monocrystalline quartz, associated with feldspar, potassium feldspar, plagioclase, and microcline. Rock fragments polycrystalline quartz, chert, opaque minerals, gypsum, mica, and heavy minerals. Planktonic & benthic foraminifera, as well as miliolids. Compaction & partial replacement by siderite, pyrite, calcite, & clay minerals. Mainly intergranular porosity	
FU9	Fine-grained Sd, well-sorted, sub-angular to sub-rounded. Linear & concave-convex, quartz grains, rock fragments, primarily sedimentary and metamorphic, few volcanic fragments. Feldspar, mainly plagioclase, carbon fibers, mica, heavy minerals, & opaque minerals, matrix consists of detrital clay & pseudomatrix, cementation by silica, kaolinite, illite, & unidentified clays, generally grow within pore spaces. Replaced by kaolinite, authigenic clay, and pyrite. Feldspar, rock fragments, mica, and carbonaceous material, mechanical and chemical compaction plays a very dominant role, intergranular porosity, dissolution secondary porosity.	
FU10	Very fine-grained Sd, sub-angular to sub-rounded, moderate sorting, elongated & point contacts. Monocrystalline quartz, K-feldspar, plagioclase, & microcline. Accessory minerals mica, carbon grains, & heavy minerals. Detrital clay & thin clay laminations. Compaction, minor cementation by clay minerals, pyrite, silica, and siderite. Intergranular pore spaces are filled & matrix and grains are replaced by clay minerals, pyrite, and siderite, as well as dissolution. Interparticle & dissolution porosity.	

rock group is expected to have its own distinct quality. In sandstone, rock texture is the main factor determining rock quality (Amaefule et al. 1993). Also, Texture is a dominant factor influencing the saturation exponent and cementation exponent (Acosta et al. 2021). The saturation exponent is higher in samples with unconnected pores and greater hydraulic unit complexity. In contrast, it tends to decrease in rock samples with connected pores, which are characterized by lower hydraulic unit complexity (Saadat et al. 2024). A plot of the resistivity index against water saturation shows a shift in slope moving to the right for lower rock quality or

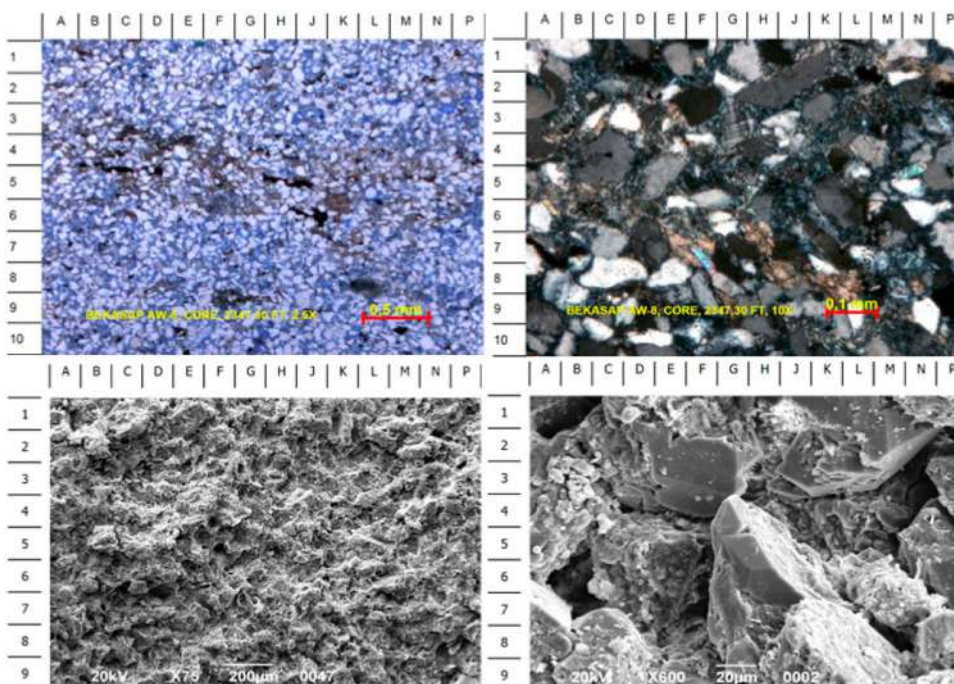
higher FU (Fig. 4). The same pattern is shown in the plot of formation factor against porosity (Fig. 5). The slope on the resistivity index plot against water saturation indicates that the saturation exponent increases as rock quality decreases. This proves a strong relationship between the global hydraulic element and the saturation exponent (Corbett and Mousa 2010). The plot of formation factor against porosity also shows a similar pattern, where the slope increases as rock quality decreases. The cementation factor varies depending on the lithology, particularly in relation to the clay content and its types (Wan Bakar et al. 2022) as well as



**Fig. 2** Petrographic analysis of rock samples for FU 1 (best quality rock group)



**Fig. 3** Petrographic analysis of rock samples for FU 10 (The worst quality rock group)



porosity types in carbonate rocks (Rostami et al. 2024). Shi-Jun demonstrated the impact of sandstone pore texture on the saturation exponent and cementation exponent (Shi-jun 2009). Several studies also indicate that the estimation of the saturation exponent ( $n$ ) and cementation exponent ( $m$ ) are influenced by rock quality (Jumaah 2021). By classifying rocks based on rock class determined by porosity, the saturation and cementation exponents can be well estimated (Venkataramanan et al. 2016).

### The influence of physical properties of rocks on rock quality and saturation exponent

The quality of rock is highly influenced by pore complexity. This pore complexity greatly determines the key physical properties of reservoir rock, such as porosity and permeability. As previously discussed, a group of rocks with the same quality exhibits similarities in shape factor and tortuosity (Amaefule et al. 1993). What differentiates them is the size

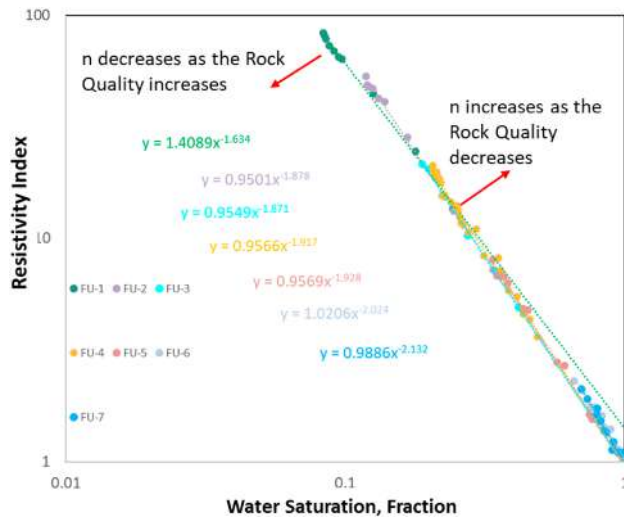


Fig. 4 Relationship between rock quality and saturation exponent

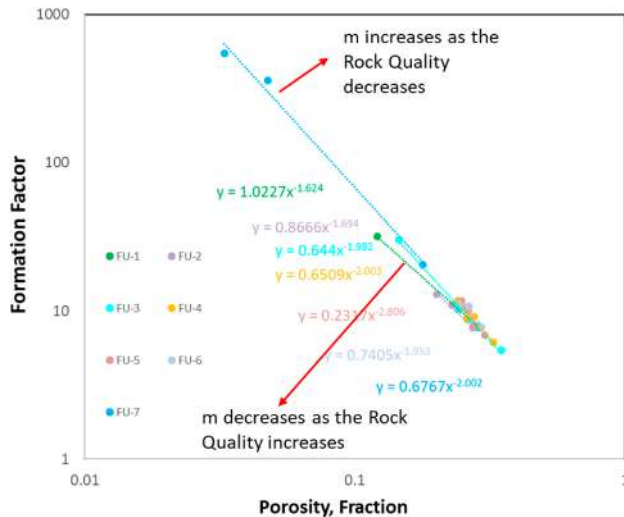


Fig. 5 Relationship between rock quality and cementation exponent

of the pore space, which is expressed as the mean hydraulic radius ( $RQI$ ). Thus, a group of rocks with the same quality should have the similar ability to transmit fluids. The ability a rock to transmit fluids is known as permeability. If permeability is influenced by pore complexity, then permeability should have an effect on the saturation exponent. Figure 6. shows the relationship between the saturation exponent and permeability, overlaid with Flow Unit (FU). Although not clearly visible, there is a certain trend of decreasing permeability with increasing saturation exponent.

Clay volume is one of the physical properties of rock that affects pore complexity. The presence of clay minerals in pore spaces varies between different types of clay. Illite and Smectite are types of clay that significantly influence pore complexity. These two minerals have a large specific surface area and a high cation exchange capacity (CEC).

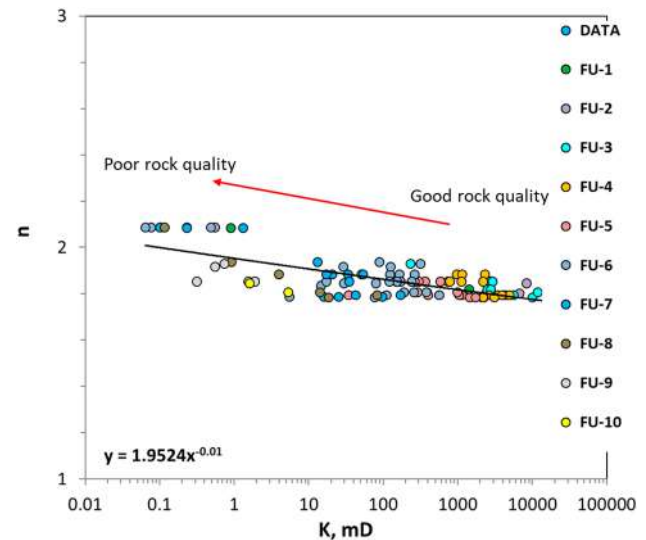


Fig. 6 Effect of permeability and rock quality on saturation exponent

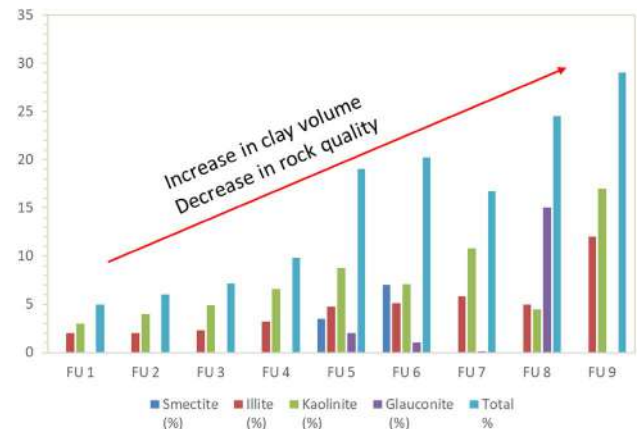


Fig. 7 Effect of clay volume on rock quality

Figure 7. shows that clay volume has a significant impact on rock quality. An increase in clay volume leads to a decrease in rock quality.

The influence of clay volume on the saturation exponent is shown in Fig. 8. An increase in clay volume leads to a decrease in rock quality and an increase in the saturation exponent. Yufei Fan demonstrated that clay volume has a significant effect on the saturation exponent (Fan et al. 2020). Figure 7. shows that clay minerals are dominated by illite and kaolinite. Lower quality rock group (larger numbers of FU), the presence of illite, glauconite, and smectite is observed to decrease rock quality. This indicates that the presence of these three minerals increases pore complexity, resulting in a higher saturation exponent. The high cation exchange capacity (CEC) of illite and smectite also contributes to the increase in the saturation exponent (Kurniawan and Bassiouni 2007).

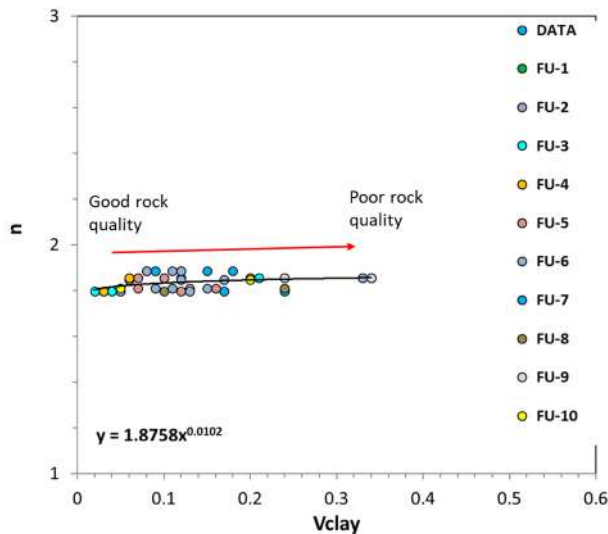


Fig. 8 Effect of clay volume on saturation exponent

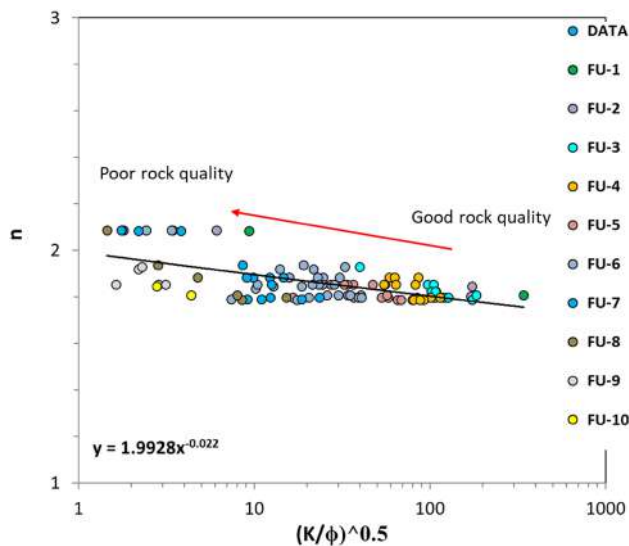


Fig. 9 Effect of pore geometry on saturation exponent

### Relationship of reservoir quality index and saturation exponent

Amaefule defined the reservoir quality index (*RQI*) using the petrophysical properties of rock porosity and permeability, expressed as  $(k/\phi)^{0.5}$  (Amaefule et al. 1993). Wibowo referred to  $(k/\phi)^{0.5}$  as pore geometry, which is comparable to the mean hydraulic radius (Wibowo and Permadi 2015). This pore geometry involves the shape and size of the pores, thereby affecting pore volume. Good quality rocks group tend to have simple pore geometry or a larger mean hydraulic radius (Prakoso et al. 2021). Pore geometry is one of the factors that causes variations in the saturation exponent (Stalheim and Eidesmo 1995; Watfa 1991). Simple geometry with larger pore size tends to indicate better quality

and generally corresponds to a lower saturation exponent (Fig. 9). On the other hand, increasingly complexity of pore geometry indicates an increase in the saturation exponent.

### Relationship of specific surface area, Kozeny constant and saturation exponent

Specific surface area is the area of the pore space wetted by fluid relative to the pore volume. Specific surface area can be approximated using the Kozeny equation (Kozeny 1927). The Kozeny equation can be rearranged as follows:

$$K = 0.9869 \frac{C\varphi^3}{S_b^2} \quad (9)$$

Equation 9 can be rearranged to estimate the specific surface area per unit bulk volume as follows:

$$S_b = \left( \frac{C\varphi^3}{K/0.9869} \right)^{0.5} \quad (10)$$

$c$  is known as the Kozeny constant. The Kozeny constant is a function of the shape factor ( $F_s$ ) and tortuosity ( $\tau$ ) (Amaefule et al. 1993). Several studies have shown that shape factor ( $F_s$ ) and tortuosity ( $\tau$ ) are two factors that influence pore complexity. The shape factor affects the shape of pores, with a value of 1 for perfectly round pores, and increases as the pore shape becomes more complex. Tortuosity ( $\tau$ ) is a parameter that also reflects pore space complexity. The more complex of the pore space, the longer of the fluid flow paths. Thus, as pore space complexity increases, tortuosity ( $\tau$ ) also increases. The Kozeny constant ( $c$ ) can be approximated using the Mortensen equation (Mortensen et al. 2007). The Mortensen equation can be expressed as follows:

$$c = \left( 4 \cos \left( \frac{1}{3} \arccos \left( \phi \frac{8^2}{\pi^3} - 1 \right) + \frac{4}{3} \pi \right) + 4 \right)^{-1} \quad (11)$$

The influence of specific surface area on rock quality and the saturation exponent is shown in Fig. 10. Rocks with good quality tend to have a low specific surface area. This is due to the simple pore shape, which is nearly perfectly round, causing the shape factor to approach 1. Simple and interconnected pore spaces result in shorter fluid flow paths and a lower tortuosity factor.

Figure 11 provides information about the influence of the Kozeny constant on saturation exponent. A low Kozeny constant characterizes by a group of rocks with simple pore shapes, resulting in a low shape factor and low tortuosity, which indicates good quality. Zhang showed that low tortuosity contributes to a decrease in the saturation exponent (Zhang et al. 2021). Figure 11 proves that the Kozeny



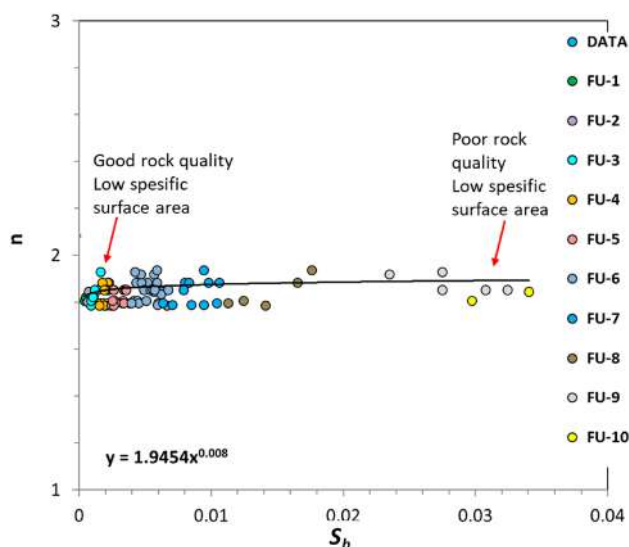


Fig. 10 Effect of specific surface area on saturation exponent

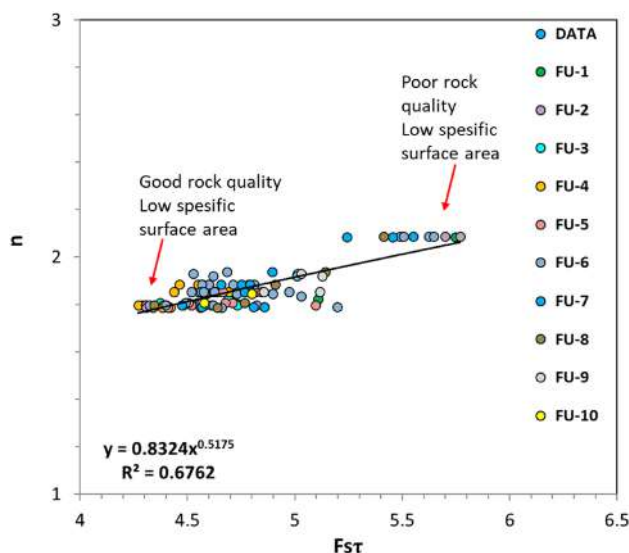


Fig. 11 Effect of Kozeny constant on saturation exponent

constant can provide an overview of rock quality and affects the saturation exponent. Good rock quality is characterized by a low Kozeny constant value and a low saturation exponent.

### Saturation exponent and water saturation estimation

Based on the previous discussion, it was found that the saturation exponent is significantly influenced by the combination of pore attributes that are shape factor and tortuosity, known as the Kozeny constant, and the physical properties of rock, specifically clay volume. A multivariate regression between the saturation exponent, Kozeny constant, and clay volume was established to obtain an empirical relationship

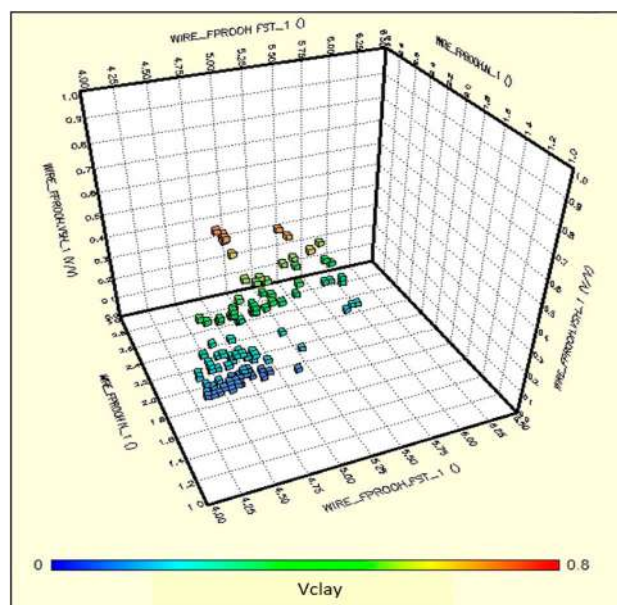


Fig. 12 Relationship between saturation exponent, Kozeny constant and clay volume

among these three parameters (Fig. 12). Based on the relationship of these three parameters, an empirical equation was derived to calculate the saturation exponent as follows:

$$n = A + (B * F_s \tau) + (C * V_{clay}) \quad (12)$$

Where  $A$ ,  $B$ , and  $C$  are empirical constants for the Kozeny constant and clay volume, whose values may vary for each field. This study obtained the constant value  $A = 0.579697$ ,  $B = 0.180011$ , and  $C = 0.126903$ . Based on Eq. 12, the saturation exponent for entire depth interval can be estimated using porosity and clay volume (Fig. 13). While the porosity and clay volume were obtained from log analysis. The log curve of the saturation exponent ( $n$ ) obtained allows for an accurate calculation of water saturation (Fig. 13). These results demonstrate that integrating porosity and clay volume data from log analyses produces a consistent and accurate estimation of water saturation for entire depth interval.

### Result validation

Validation was performed by comparing the calculated water saturation with the water saturation data from the core (Figs. 14, 15 and 16). The water saturation estimated using the varying saturation exponent value yielded good results. Qualitatively, the calculated saturation results closely match the water saturation data from laboratory measurements (Figs. 14A, 15A and 16A). The plot comparing measured and calculated water saturation, although still somewhat scattered, shows a trend that follows the line represented by the equation  $Y = X$  (Figs. 14B, 15B and 16B).



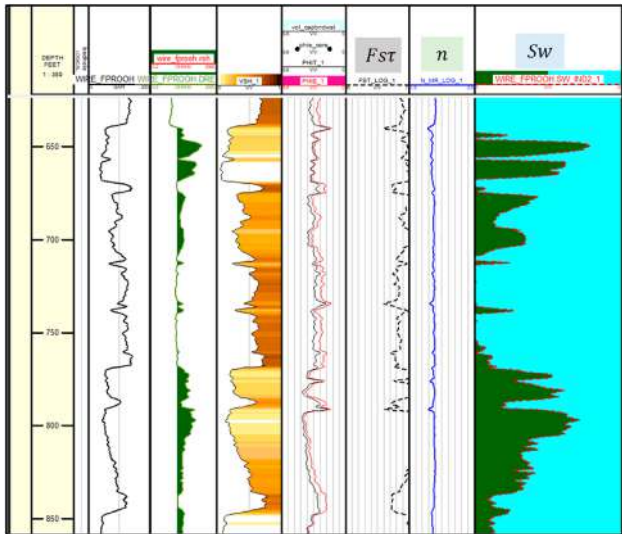


Fig. 13 Results of estimating the saturation exponent and water saturation calculation

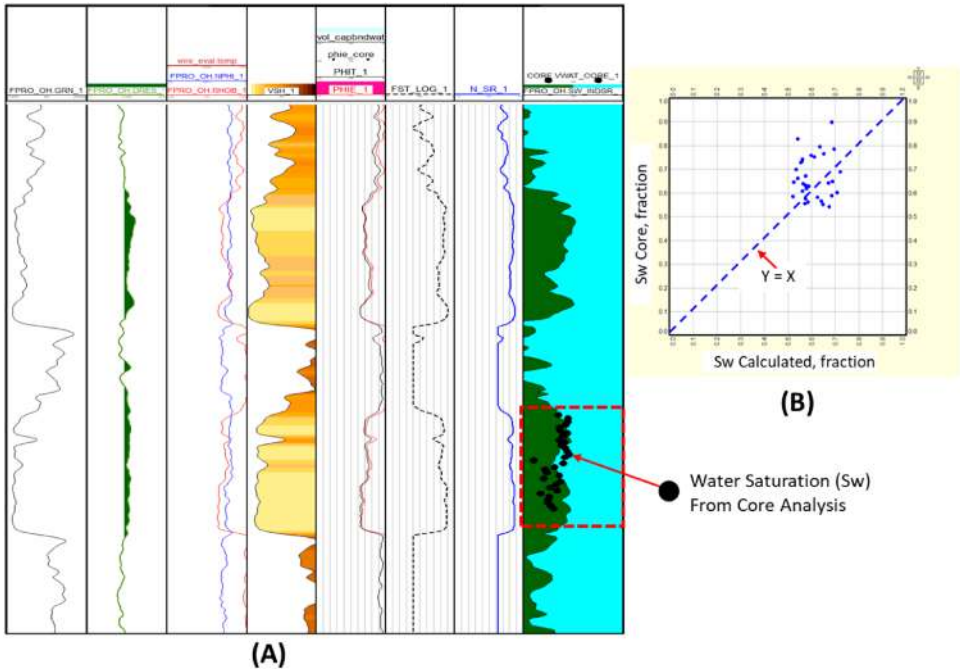
These results show that this study provides additional knowledge to the understanding of the relationship between pore quality and saturation exponent in water saturation calculations, especially in heterogeneous reservoir rocks. The findings show that the saturation exponent is not only influenced by the type of lithology, but also by the pore complexity. The approach of varying saturation exponent values for the entire reservoir can produce more accurate water saturation calculations. This study adds new understanding and a simple approach in estimating the saturation exponent required for water saturation calculations.

## Conclusions

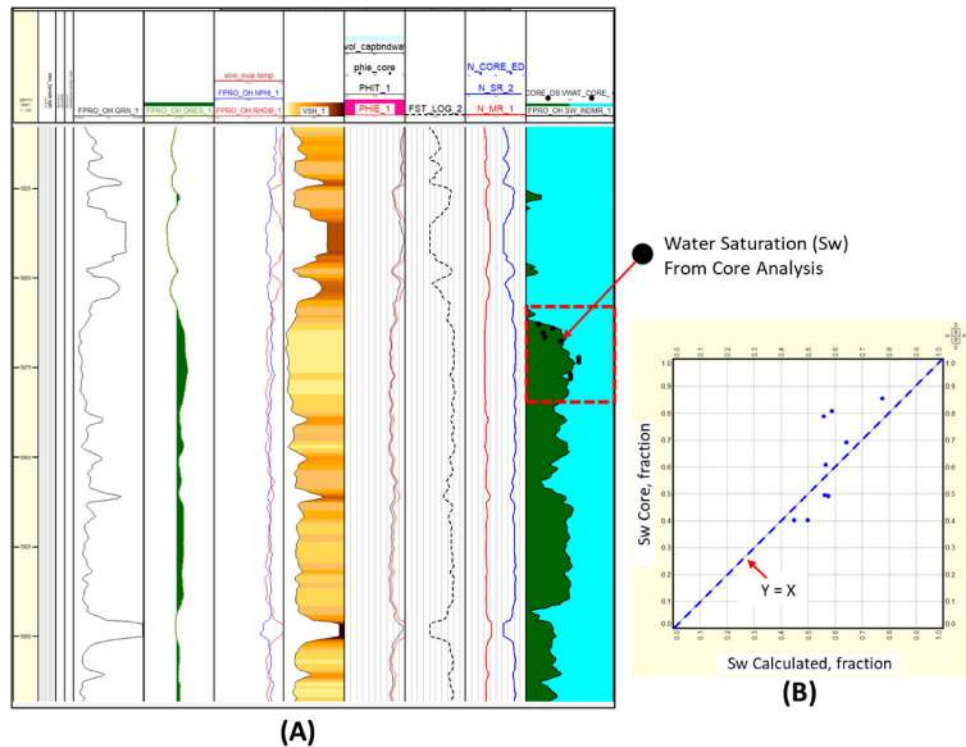
Some conclusions obtained from this study are as follows:

1. In sandstone, the study of factors affecting rock quality (texture, porosity, and clay volume) revealed a negative relationship with the saturation exponent. The saturation exponent is lower for good rock quality, and a decrease in rock quality leads to an increase in the saturation exponent.
2. Flow unit-based observations show that the saturation exponent value increases with increasing flow unit numbers, indicating increasing pore complexity and decreasing rock quality. This decreasing rock quality is also shown in the relationship between permeability and clay volume with the saturation exponent, where decreasing permeability and increasing clay volume will increase the saturation exponent.
3. The reservoir quality index is an indicator of rock quality. The saturation exponent tends to be higher for rocks with a low reservoir quality index. The reservoir quality index is defined as a function of the pore shape factor and tortuosity.
4. The combination of the pore shape factor and tortuosity is widely known as the Kozeny constant. Considering that clay volume is one of the factors affecting rock quality, an empirical equation between the combination of pore shape factors and tortuosity attributes and clay volume with saturation exponent can be arranged.
5. The saturation exponent for the entire depth interval can be predicted well using the empirical equation obtained

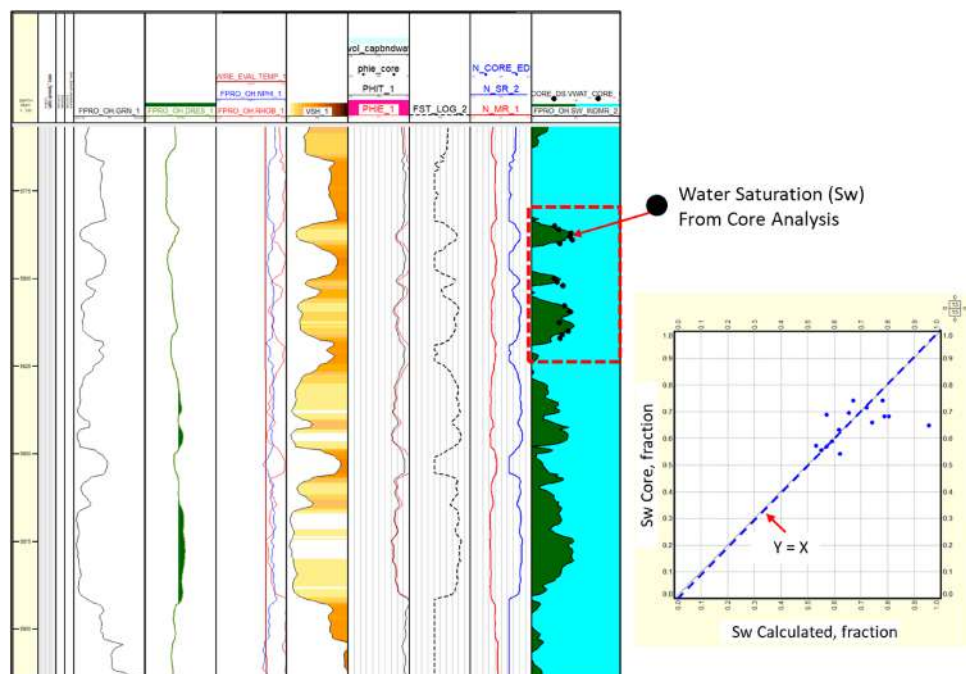
Fig. 14 Validation of water saturation calculation results of well A



**Fig. 15** Validation of water saturation calculation results of well B



**Fig. 16** Validation of water saturation calculation results of well C



from this study (Eq. 12). The combination of pore shape factor and tortuosity can be calculated from porosity, while porosity and clay volume can be easily obtained from log analysis.

**Acknowledgements** We would like to thank the Ministry of Education, Culture, Research and Technology, LLDIKTI III and Institution of Research and Community Services Universitas Trisakti for their valuable support and assistance in this study. We are also grateful to

the optical petrography and mineralogy laboratory and core analysis laboratory, Faculty of Earth and Energy Technology for provided petrography analysis and core analysis data for this research work.

**Funding** This research was funded by the Indonesian Ministry of Education, Culture, Research and Technology, LLDIKTI III (2024) through competitive research grant under the Fundamental Research Scheme, contract number 832/LL3/AL.04/2024 & 180/A/LPPM-P/USAKTINI/2024. We appreciate for the financial support from these funding agencies.

## Declarations

**Conflict of interest** On behalf of all the co-authors, the corresponding author states that there is no conflict of interest.

**Open Access** This article is licensed under a Creative Commons Attribution-NonCommercial-NoDerivatives 4.0 International License, which permits any non-commercial use, sharing, distribution and reproduction in any medium or format, as long as you give appropriate credit to the original author(s) and the source, provide a link to the Creative Commons licence, and indicate if you modified the licensed material. You do not have permission under this licence to share adapted material derived from this article or parts of it. The images or other third party material in this article are included in the article's Creative Commons licence, unless indicated otherwise in a credit line to the material. If material is not included in the article's Creative Commons licence and your intended use is not permitted by statutory regulation or exceeds the permitted use, you will need to obtain permission directly from the copyright holder. To view a copy of this licence, visit <http://creativecommons.org/licenses/by-nc-nd/4.0/>.

## References

- Abu-Hashish MF, Afify HM (2022) Effect of petrography and diagenesis on the sandstone reservoir quality: a case study of the middle miocene Kareem formation in the North geisum oil field, Gulf of suuez, Egypt. *Arab J Geosci* 15(6):465. <https://doi.org/10.1007/s12517-022-09686-z>
- Abu-Hashish MF, Ali SB (2021) Integration of well logs and seismic data for facies analysis and modelling of the El-Wastani Formation in the Sequoia Gas Field, offshore Nile Delta, Egypt. *J Afr Earth Sci*. <https://doi.org/10.1016/j.jafrearsci.2021.104343>
- Abu-Hashish MF, Al-Sharif AW, Hassan NM (2022) Hydraulic flow units and reservoir characterization of the Messinian Abu Madi Formation in West El Manzala Development Lease, onshore Nile Delta, Egypt. *J Afr Earth Sc*. <https://doi.org/10.1016/j.jafrearsci.2022.104498>
- Acosta ER, Nandlal B, Harripersad R (2021) Saturation exponent as a function of reservoir heterogeneity and wettability in the Tambaredjo Oil Field, Suriname. SPWLA 62nd Annual Online Symposium Transactions. <https://doi.org/10.30632/SPWLA-2021-0118>
- Adisoemarta PS, Anderson GA, Frailey SM, Asquith GB (2001) Saturation exponent  $n$  in well log interpretation: another look at the permissible range. *Soc Petroleum Eng - SPE Permian Basin Oil Gas Recovery Conf 2001 OGR 2001*. <https://doi.org/10.2118/70043-ms>
- Al-Dujaili AN (2023) Reservoir rock typing and storage capacity of Mishrif carbonate formation in West Qurna/1 Oil Field, Iraq. *Carbonates Evaporites*. <https://doi.org/10.1007/s13146-023-00908-3>
- Al-Dujaili AN, Shabani M, AL-Jawad MS (2021) Characterization of flow units, rock and pore types for Mishrif Reservoir in West Qurna oilfield, Southern Iraq by using lithofacies data. *J Petroleum Explor Prod Technol*. <https://doi.org/10.1007/s13202-021-01298-9>
- Al-Dujaili AN, Shabani M, AL-Jawad MS (2023) Effect of heterogeneity on capillary pressure and relative permeability curves in carbonate reservoirs. A case study for Mishrif formation in West Qurna/1 Oilfield, Iraq. *Iraqi J Chem Petroleum Eng*. <https://doi.org/10.31699/ijcpe.2023.1.3>
- Al-Hilali MM, Al-Abideen MJZ, Adegbola F, Li W, Avedisian AM (2015) A petrophysical technique to estimate archie saturation exponent ( $n$ ); Case studies in carbonate and shaly-sand reservoirs - IRAQI oil fields. *Society of Petroleum Engineers - SPE Annual Caspian Technical Conference and Exhibition, CTCE 2015*. <https://doi.org/10.2118/177331-ms>
- Al-Otaibi MH, Khamatdinov R, Al-Khaldi N, Abdelrahim R, Bouaouaja M (2012) Water saturation modeling in Khafji carbonate reservoir. *Society of Petroleum Engineers - Abu Dhabi International Petroleum Exhibition and Conference 2012, ADIPEC 2012 - Sustainable Energy Growth: People, Responsibility, and Innovation, 2*. <https://doi.org/10.2118/161427-ms>
- Amaefule JO, Altunbay M, Tiab D, Kersey DG, Keelan DK (1993) Enhanced reservoir description: using core and log data to identify hydraulic (Flow) units and predict permeability in uncored intervals/Wells. *SPE Annual Tech Conf Exhib*. <https://doi.org/10.2118/26436-MS>
- Ara TS, Talabani S, Atlas B, Vaziri HH, Islam MR (2001) In-depth investigation of the validity of the archie equation in carbonate rocks. *Proceedings-SPE production operations symposium*. <https://doi.org/10.2118/67204-ms>
- Archie GE (1942) The electrical resistivity log as an aid in determining some reservoir characteristics. *SPE Reprint Series*. <https://doi.org/10.2118/942054-g>
- Chen X, Kuang LC, Sun ZC (2002) Archie parameter determination by analysis of saturation data. *Petrophysics*, 43(2)
- Corbett PWM, Mousa NIA (2010) Petrotype-based sampling applied in a saturation exponent screening study, Nubian sandstone formation, Sirt basin, Libya. *Petrophysics*, 51(4)
- Donaldson EC, Siddiqui TK (1989) Relationship between the Archie saturation exponent and wettability. *SPE Form Eval*. <https://doi.org/10.2118/16790-pa>
- El-Khatib N (1995) Development of a modified capillary pressure J-Function. *Spe*, 547–562
- Fan Y, Pan B, Guo Y, Lei J (2020) Effects of clay minerals and Pore-Water conductivity on saturation exponent of clay-bearing sandstones based on digital rock. *Petrophys-SPWLA J Format Eval Reserv Descr* 61(04):352–362. <https://doi.org/10.30632/PJV61N4-2020a2>
- Hamada GM, AL-Awad MN, Alsughayer A (2002) Variable saturation exponent effect on the determination of hydrocarbon saturation. *All Days*. <https://doi.org/10.2118/77887-MS>
- Jumaah HA (2021) Modified Archie's parameters for estimating water saturation for carbonate reservoir in north of Iraq. *J Petroleum Explor Prod Technol*. <https://doi.org/10.1007/s13202-021-01258-3>
- Kozeny J (1927) Über kapillare Leitung des wassers Im Boden. *Akad Wiss Wien* 136:271–306
- Kumar M, Senden TJ, Sheppard AP, Arns CH, Knackstedt MA (2010) Variations in the archie's exponent: Probing wettability and low sw effects. *SPWLA 51st annual logging symposium 2010*
- Kurniawan B, Bassiouni Z (2007) Use of cec-dependent cementation and saturation exponents in shaly sand resistivity models. *48th annual logging symposium 2007*
- Mortensen J, Engstrom F, Lind I (2007) The relation among porosity, permeability, and specific surface of chalk from the gorm field, Danish North sea. *SPE Reservoir Eval Eng*. <https://doi.org/10.2118/31062-pa>
- Olusola BK, Aguilera R (2013) How to estimate water saturation exponent in dual and triple porosity reservoirs with mixed wettability. *Society of petroleum engineers-SPE Canadian unconventional resources conference 2013-unconventional becoming conventional: lessons learned and new innovations, 2*. <https://doi.org/10.2118/167213-ms>
- Prakoso S, Burhannudinnur M, Irham S, Rahmawan S, Yasmaniar G (2021) Linkage of cementation factor on rock quality in sandstone. *AIP Conf Proc*. <https://doi.org/10.1063/5.0061148>
- Rabiee R, Hamada G (2022) Artificial neural network modeling for water saturation determination in Shaly sandstone reservoirs:

- case study Egyptian oil field. SSRN Electron J. <https://api.semanticscholar.org/CorpusID:246988787>
- Rostami A, Helalizadeh A, Moghaddam MB, Soleymanzadeh A (2024) New insights into estimating the cementation exponent of the tight and deep carbonate pore systems via rigorous numerical strategies. *J Petroleum Explor Prod Technol* 14(6):1605–1629. <https://doi.org/10.1007/s13202-024-01776-w>
- Saadat K, Rahimpour-Bonab H, Tavakoli V, Gholinezhad J (2024) Experimental investigation and prediction of saturation exponent in carbonate rocks: the significance of rock-fluid properties. *J Petroleum Explor Prod Technol*. <https://doi.org/10.1007/s13202-023-01714-2>
- Shi-jun Y (2009) Influence of sandstone pore texture on cementation exponent and saturation error analysis in Kuche Area, Tarim Basin. *Well Logging Technology*. <https://api.semanticscholar.org/CorpusID:131019560>
- Sondena E, Brattell F, Kolltvelt K, Normann HP (1992) Comparison between capillary pressure data and saturation exponent obtained at ambient conditions and at reservoir conditions. *SPE Form Eval*. <https://doi.org/10.2118/19592-pa>
- Stalheim SO, Eidesmo T (1995) Is the saturation exponent  $n$  a constant? SPWLA 36th annual logging symposium 1995
- Tiab D, Donaldson EC (2015) *Petrophysics: theory and practice of measuring reservoir rock and fluid transport properties: Fourth Edition*. In *Petrophysics: theory and practice of measuring reservoir rock and fluid transport properties: Fourth Edition*. <https://doi.org/10.1016/C2014-0-03707-0>
- Tian J, Wang L, Rong Zhao R, Liu H, Qi Zhang Q, Sim H, Qiang L (2022) Improved triple porosity model for calculating porosity exponent of fractured-vuggy reservoirs based on Maxwell-Garnett mixing rule and anisotropic conductivity analysis. *J Petrol Sci Eng*. <https://doi.org/10.1016/j.petrol.2022.110265>
- Tian J, Wang L, Ostadhassan M, Zhang L, Liu H, Sima L (2024) Pore structure exponent of Archie's law in a dual-porosity medium: Vuggy reservoirs. *Geoenergy Sci Eng*. <https://doi.org/10.1016/j.geoen.2024.212659>
- Venkataramanan L, Donadille JM, Reeder SL, Van Steene M, Gkortsas VM, Fellah K, Ramsdell D, Al-Rubaiyea JA, Al-Ajmi FA, Al-Houli M, Wilkinson P, Bajunaid H (2016) A new method to estimate cementation and saturation exponents from dielectric dispersion data. *Proc-SPE Annual Tech Conf Exhib*. <https://doi.org/10.2118/181451-ms>
- Wan Bakar WZ, Saaid M, Ahmad I, Amir MR, Japperi Z, Ahmad Fuad MFI (2022) Improved water saturation estimation in shaly sandstone through variable cementation factor. *J Petroleum Explor Prod Technol*. <https://doi.org/10.1007/s13202-021-01391-z>
- Watfa M (1991) Using electrical logs to obtain the saturation exponent ( $n$ ) in the Archie equation. *Proc Middle East Oil Show*. <https://doi.org/10.2523/21415-ms>
- Wibowo AS, Permadi P (2015) A type curve for carbonates rock typing. <https://doi.org/10.2523/iptc-16663-ms>
- Worthington PF, Pallatt N (1990) Effect of variable saturation exponent upon the evaluation of hydrocarbon saturation. *Proc-SPE Annual Tech Conf Exhib Omega*. <https://doi.org/10.2118/20538-ms>
- Yadav L, Singh A, Dasgupta T (2017) Experimental basis for prediction of cementation, water saturation and bound water volume exponents with grain size variation in fresh water fluvial reservoirs
- Zhang Z, Liu L, Li C, Cai J, Ning F, Meng Q, Liu C (2021) Fractal analyses on saturation exponent in Archie's law for electrical properties of hydrate-bearing porous media. *J Petrol Sci Eng*. <https://doi.org/10.1016/j.petrol.2020.107642>

**Publisher's note** Springer Nature remains neutral with regard to jurisdictional claims in published maps and institutional affiliations.